Accepted Manuscript

Geological Society, London, Special Publications

Unusual sauropod slipping tracks preserved on a biostabilized tidal flat from the Lower Cretaceous of northern Patagonia, Argentina

Arturo M. Heredia, Pablo J. Pazos & Diana E. Fernández

DOI: https://doi.org/10.1144/SP522-2021-136

To access the most recent version of this article, please click the DOI URL in the line above. When citing this article please include the above DOI.

Received 13 August 2021
Revised 29 April 2022
Accepted 6 May 2022

Unusual sauropod slipping tracks preserved on a biostabilized tidal flat from the Lower Cretaceous of northern Patagonia, Argentina

Arturo M. Heredia[1, 2, *], Pablo J. Pazos[1, 2], Diana E. Fernández[1, 2]

[1] Universidad de Buenos Aires, Facultad de Ciencias Exactas y Naturales, Departamento de Ciencias Geológicas, Buenos Aires, Argentina

[2] CONICET - Universidad de Buenos Aires, Instituto de Estudios Andinos Don Pablo Groeber (IDEAN), Buenos Aires, Argentina

ORCID ID: A.M.H., 0000-0001-8140-9921; P.J.P., 0000-0003-3728-6906; D.E.F, 0000-0002-3931-3093

*Corresponding author (e-mail address: heredia@gl.fcen.uba.ar)

Abstract

Several elongated and other crescent-shaped impressions interpreted as dinosaur tracks and preserved on Lower Cretaceous tidal flat deposits from the Agrio Formation (northern Patagonia, Argentina) are studied in detail. These tracks were documented on a palaeosurface showing palaeotopographic differences over a short distance, related to the lateral migration of a tidal channel. A genetic order between biostabilization and bioturbation of the palaeosurface is recognized. Ripples generated within the channel during the flood tide were first biostabilized; there, horseshoe crab trace fossils were produced. Then, the area bearing the tracks studied here was subaerially exposed, with the biostabilized substrate generating a slippery surface. Scanning electron microscope (SEM) analysis of the rims indicates that the microbial mat was disturbed by the trampling. Finally, microbial mats recovered, and some tracks preserve wrinkle marks inside the tracks. Taking into account the substrate properties and track features analized (morphology, size, depth, and orientation), it is concluded that the tracks were produced by dinosaurs, probably small sauropods, trampling on a slippery surface and moving parallel to the channel margin. This study is an unusual case of slipping tetrapod tracks preserved on a biostabilized tidal flat developed in a mixed carbonate-siliciclastic environment.

Tidal flats are complex environments influenced by tidal fluctuations, fluvial discharges, other coastal processes, as well as waves and storms, and climate seasonal variability, where the sedimentary processes change from a single day up to tidal cycles. The interaction of these factors affects the characteristics of the deposited sediments (e.g. lithology, thickness), the timing and nature of subaerial exposure, the development of microbial mats, and the preservation of trace fossils in both, recent and ancient records. Bioestabilised substrates, in particular, play a key role in track preservation, as has been observed from dinosaur tracksites from marginal-marine or fluvial palaeoenvironments (de Souza Carvalho *et al*. 2013; Dai *et al*. 2015; Paik *et al*. 2017; Xing *et al*. 2019; Heredia *et al*. 2020).

The morphology of tetrapod tracks is related to both anatomical features and locomotor dynamics of the trackmaker and is also strongly determined by physical properties of the underlying substrate, such as grain size, moisture content, and composition (Manning 2004; Milàn and Bromley 2008; Díaz-Martínez *et al*. 2009; Marty *et al*. 2009; Platt *et al*. 2012; Falkingham 2014). Microbial mats are capable of modifying substrate behavior through binding and stabilizing sand-sized grains, which could play a key role in defining the final morphology and preservation of trace fossils (e.g. Noffke *et al*. 2001; Marty *et al*. 2009; Fernández and Pazos 2013). Actualistic experiments on the interaction of microbial mats and the formation and ichnotaphonomy of tetrapod tracks are uncommon and have been carried out on present-day siliciclastic tidal flats, including implications for the study of the track record (Marty *et al*. 2009; Carmona *et al*. 2012; Cuadrado *et al*. 2021). Whereas neoichnological studies exploring the track preservation in carbonate and mixed carbonate-siliciclastic tidal flats are absent and could contribute in the future to the understanding of ancient track interpretations such as those in the present work.

The Neuquén Basin is a good example of a basin where marginal marine siliciclastic, but also mixed carbonate-silicicastic facies coexisted in the Early Cretaceous. In the Agrio Formation, in particular, a robust palaeoenvironmental framework based on

sedimentological, stratigraphical, and palaeontological studies included significant information about ichnology. Palaeoenvironmental refinement and high-frequency changes in stratigraphic architecture were presented (e.g. Spalletti *et al*. 2001; Lazo *et al*. 2005; Archuby and Fürsich 2010; Cichowolski *et al*. 2012; Schwarz *et al*. 2018). In the Agrio Formation, ichnological investigations have been mainly related to invertebrate ichnology (e.g. Pazos 2009, 2011; Pazos and Fernández 2010; Fernández *et al*. 2010, 2018, 2019; Fernández and Pazos 2012, 2013, 2015; Giachetti *et al*. 2020; Andrada *et al*. 2020). Consequently, knowledge about the record of vertebrate tracks in marginal marine facies of the unit is limitedand related to mixed siliciclastic-carbonate deposits evidencing subaerial exposure in unknownareas of the basin (e.g. Pazos *et al*. 2012a, 2020; Heredia *et al*. 2018). This study provides an in-depth analysis of several flattened, elongated and other crescent-shaped impressions, documented in marginal marine deposits related to tidal influence in the uppermost part of the Agrio Formation (Agua de la Mula Member). They were briefly analysed and preliminarily assigned to vertebrate tracks by Pazos *et al*. (2012b).

The aims of this work are: to describe and interpret in detail several impressions and reconstruct the lateral variability of a palaeosurface that documents palaeotopographic differences within a short distance; to analyse the role played by the substrate consistency (including biostabilisation) in the morphology and final preservation of the impressions (interpreted as tracks); and to discuss a possible producerand other palaeoecological inferences.

Geological setting

The Neuquén Basin, located in west-central Argentina and Chile, extends from 32° to 40° S latitude along the Andean foothills and forms a large NW-SE orientated marine embayment (Fig. 1A). It is filled by a continuous Late Triassic–Palaeogene stratigraphic record of marine to continental settings more than 7000 m thick (Legarreta and Gulisano 1989; Vergani *et al*. 1995; Howell *et al*. 2005). This basin records a complex tectonic evolution, starting with an initial Late Triassic–Early Jurassic syn-rift stage, followed by a

Middle Jurassic–Early Cretaceous thermal subsidence regime in a retroarc setting, and concluding as a Late Cretaceous–Palaeogene foreland basin system (Manceda and Figueroa 1995; Howell *et al*. 2005; Naipauer and Ramos 2016; Fennell *et al*. 2020).

The Agrio Formation (Weaver 1931) is late Valanginian–latest Hauterivian in age (Aguirre-Urreta *et al*. 2019) and is the uppermost unit (Fig. 1B) within the Upper Jurassic–Lower Cretaceous Mendoza Group (Groeber 1946). Stratigraphically, this unit is located above the continental to marginal-marine succession of the Mulichinco Formation (early Valanginian) and is unconformably overlain by Barremian–Aptian continental, marine, and marginal-marine deposits included in the Huitrín Formation (Legarreta 2002; Lazo and Damborenea 2011). The Agrio Formation comprisesthree members (Fig. 1B), which are, in stratigraphic order, the Pilmatué, Avilé, and Agua de la Mula members (Weaver 1931; Leanza *et al*. 2001). The lower and upper members are marine and the Avilé Member is a fluvio-aeolian system deposited during a forced regression in the middle Hauterivian (Veiga *et al*. 2007). Recently, several stratigraphic sequences have been recognized for the first time for the Pilmatué Member, and the previously mentioned forced regression was related to a tectonic origin rather than a classical eustatic interpretation (Pazos *et al*. 2020). In agreement with the previous suggestion of Guler *et al*. (2013), four fourth-order sequences were recognized in the Agua de la Mula Member in a new sequence stratigraphic interpretation for the entire unit proposed by Pazos *et al*. (2020).

The Agua de la Mula Member was interpreted as a storm-dominated, mixed carbonate-siliciclastic ramp (e.g. Spalletti *et al*. 2001; Lazo *et al*. 2005; Comerio *et al*. 2018) that evolved to a marginal-marine environment containing different indicators of tidal controls such as inclinated heterolithic stratification (IHS), bidirectional orientationsin climbing ripples, and rythmites (e.g. Pazos and Fernández 2010; Pazos *et al*. 2012a; Fernández and Pazos 2012, 2013). The uppermost part of the unit with the widespread marginal-marine deposits indicates the end of a depositional cycle at basin scale (Pazos *et al*. 2020). In the locality of Cerro Rayoso (Fig. 1A), in the uppermost levels of this member (Figs. 1B, 2), is where the trace fossils analysed in this paper occur. They are found only a couple of metres laterally to

the xiphosuran trackways studied by Fernández and Pazos (2013); that area was interpreted by the authors as the record of a high-tide mating ground on a tidal flat.

Materials and methods

The study area outcrops to the east of the National Road 40, between Zapala and Chos Malal cities in the Neuquén Province (Fig. 1A). A GPS point is given as reference of the trace-fossil bearing level: 37° 44′ 54″ S, 69° 56′ 9″ W.

The present study material consists of several impressions, i.e. a mark made on the surface of something by pressing an object on it, and we have then interpreted them as tracks (see Section "Discussion: Producer"). Even though the term “impression” is more descriptive than “track”, it has been decided to homogenise the use of the terms throughout the manuscript by using only the term track, which is also more practical and comfortable for a smoother reading.

In the study, elongated tracks were considered those with a length/width ratio greater than 2. Also, to calculate individual trace fossil areas and the surface bioturbation index (the ratio between the area of the track-bearing surface and the area covered by the tracks), the public domain, java-based image processing program ImageJ was used. This is the equivalent of the concept proposed by Lockley and Conrad (1989) as the dinoturbation index that considers the surface percentage of substrate impacted by dinosaurs.

The photogrammetric 3D models have been obtained using Agisoft Metashape 1.5.0 Professional Edition (Educational License) following the procedures indicated by Falkingham (2012). The false-depth colour images and contour lines were produced with the free software Paraview (www.paraview.org).

Vertical sections of the uppermost millimetres of the track-bearing surface were analysed under scanning electron microscope (SEM; Zeiss Supra 40 with ultrahigh-resolution field-emission scanning) and photographed (see Section “Substrate analysis and ichnotaphonomy”) at magnifications from 2,000× to 20,000× using standard sample preparation (thin gold coat).

The track-bearing palaeosurface

The track-bearing palaeosurface herein studied is located 12 metres below the top of the Agua de la Mula Member (Fig. 2) in the eastern flank of the Cerro Rayoso anticline and the surface containing the tracks is laterally equivalent to the one described by Fernández and Pazos (2013), just a couple of metres aside. On the opposite flank of the anticline, Tunik *et al*. (2009) described tidal-related features, subaerial exposure, and dinosaur tracks in oolitic strata, exactly in the same stratigraphic uppermost part of the unit. These levels were documented in the assumed centre of the basin were no subaerial exposure had been recognized before (e.g. Legarreta 2002). Later, in the same locality studied here, but in underlying levels, oolitic shoal bars, tidal reactivation surfaces with mud drapes, abundant dinosaur tracks and trackways, and microbial mat-related structures were reported by Pazos *et al*. (2012a). All these data permitted to these authors to conclude that the final stage of deposition of the Mendoza Group presentsminor bathymetric differences betweenthe basin border and the basinal areas, indicating overall desiccation in almost the entire basin (Pazos *et al*. 2020, fig. 8). In particular, in the study area, Pazos *et al*. (2012b) documented a distinct palaeotopography in the level bearing the tracks described in this paper taking into account an inclined surface covered by ripples that pass laterally to channelled deposits or an almost horizontal surface with flat-topped ripples. For this reason, the track-bearing palaeosurface is analized in laterally contiguously defined sections (A–D). The zones A–D are oriented approximately south-north. The palaeosurface is clearly visible in the Fig. 3A–F, besides a vertical section showing lateral accretion features is also documented (Fig. 3G). The reconstruction of the lateral extended palaeosurface is schematized in the Fig. 4 to account the extremely short distance variability in sedimentary features and trace fossils.

Zone A

Description

This zone is almost flat, not well exposed by debris and vegetation. There, patchily carbonate levels with yellow-orange colour containing polygonal forms resembling mud cracks are exposed. They present vertical borders and bubble-like subcircular domed areas

in the central part of polygons. The border, rather than constrasting infilling is a vertical curved expression of the same material. There, the nature of the lamination is visible in the vertical walls (Fig. 3A). In the same section and in the same stratigraphic position, carbonate laminites were documented in surface in the other flank of the anticiline (Tunik *et al*. 2009) and also in underlying levels of the study locality (Pazos *et al*. 2021). Fernández and Pazos (2013) document several levels with carbonates indicating periods of active carbonate precipitation and others with more siliciclastic supply.

Interpretation

Fernández and Pazos (2013) interpreted these cracks as dissecated microbial mats. The carbonate composition, the uplifted borders and the bubble-like forms are frequent in upper inter to supratidal zone where evaporation is greater than in other zones and microbial biostabilized surfaces are prone to cracking (Bose and Chafetz 2009). The complete absence of bioturbation point out to hostile conditions and isolation of the surface with the undermat zone.

Zone B

Description

This zone is topographically depressed with respect to the remaining zones. It is completely siliciclastic in nature and exhibits an orientationE-W with an asymmetrical cross-section being almost vertical in contact with the Zone A and a gently inclined surface in the transition with the Zone C. The depression is approximately 0.5 m in depth with the deepest area close to de vertical contact, and in the middle of the depression a trend of ripples is preserved at the base. These ripples exhibit a remarkable asymmetry profile were abundant invertebrate ichnofossils were documented by Fernández and Pazos (2013). The most notable ichnogenus is *Kouphichnium* Nopcsa 1923 attributed to xiphosurans. Other trace fossils include burrows produced by vermiforms producers, such as specimens belongs to *Cochlichnus* Hitchcock 1858 and *Gordia* Emmons 1844 ichnogenera (Fernández and Pazos 2013, fig. 7D–F). More interestingly, the ripples exhibit a lee side with an abnormally high angle, and delicate trace fossils by vermiform producers are preserved (Fernández and

Pazos 2013, fig. 7 E–F). It suggests that the ripples were not active due to a very high angle of repose, and pristine preservation of trace fossils indicates a mechanism of stabilization before bioturbation rather a souply substrate. Some ripple crests are eroded (flat-topped) as well as bioturbation (Fernández and Pazos 2013, fig. 4 and 6). Also, parallel line marks have been documented along the side of some ripples (Fig. 3D) that indicates the water level position. It has also been documented in many modern tidal flats, such as in the Mont Saint Michael in France (Fig. 3E).

The gently inclined surface that is the other limit of the depression or Zone B contains ripples with the same orientation and features than the described before, but with subtle differences. For instance the high is reduced and not bioturbation or erosion was documented (Figs. 4, 5). They represent the lateral continuity of the same trends and were generated by flow with the same orientation.

Interpretation

Sedimentologically the Zone B and the transition with the Zone C is interpreted as a palaeochannel. The asymmetry and the lateral accretion surfaces observed in cross-section (Fig. 3G, 4) indicates the development of a point bar. This channel is interpreted as the result of tidal activity, in a tidal flat. The flood dominated ripple orientation points out a remarkable asymmetry in the tidal cycle. Notably, the absence of erosion of the ripples in the inclined surface, suggest that the maximum tidal level exeded the tidal channel limits. They were generated by currents that were more energetic than others during tidal recess. The orientation of the ripples and the channel is in agreement with the E-W deepening basin trend (Fig. 1A) envisaged in the literature for the Agrio Formation (e.g. Legarreta 2002). Moreover, the tidal activity is in agreement with the widespred tidal evidences in the basin documented by Pazos *et al*. (2020) in the uppermost part of the unit. The erosion ripples and the parallel lines deserves an special explanation. During the tidal ebb, only after the water flowed into the channel to the open sea, the energy was enough to eroded the ripple crests. At the same time the inclined side of the channel was exposed and wet, as not cracking was documented. The entire scenario, suggests a highly dynamic environment, as microbial mats

usually demands several days for its development (Marty *et al*. 2009; Carmona *et al*. 2012; Cuadrado *et al*. 2021). In modern tidal flats, vegetation sometimes also reduces the tidal ebb energy (Bradley *et al*. 2018). Considering that xiphosurans usually migrate to tidal areas by matting (Fernández and Pazos 2013 and reference therein), the documented xiphosuran trace fossils suggest that the channels may have been suitable corridors for these arthropods. The parallel lines in the lateral steeply side of the ripples clearly indicates the lowermost level of the water table into the channel. Al least for a pre-stabilization surface. The stabilization of the substrate by microbial mats was infered by Fernández and Pazos (2013) on the basis of the presence of wrinkle marks on top of ripples and detailed SEM observations, where vertically oriented sheaths were documented (Fernández and Pazos, 2013, fig. 8).

Zone C

Description

This zone is the lateral continuation of the inclined surface and it is almost horizontal. It is the zone that contains the impresisons analysed in this paper (Figs. 5, 6, 7) that will be described in the Section “Ichnology”. Wrinkle marks are preserved inside the tracks (Fig. 3F) and also laterally to them. Almost any other macroscopic feature is observable, the tracks present rims that were analysed in detailed by SEM (see Section “Substrate analysis and ichnotaphonomy”).

Interpretation

The existence of wrinkle marks inside the tracks indicates that residual water permitted the mat to recover after tracks. Both the SEM analysis of the rims and the slippery surface developement for this zone will be discussed in the Section “Substrate analysis and ichnotaphonomy” as well as the orientation with respect to the channel (Zone B) of the tracks.

Zone D

Description

This zone extends laterally to Zone C in the opposite direction of Zone B (Fig. 4). It is a relatively flat area; however, detailed observation permitted to recognize extremely eroded ripples, where only the troughs are preserved and oriented with similar axes than in the other zones (Figs. 4, 8). Inside some of them, corrugations (wrinkle marks) and also some tracks and silicified wood remains oriented parallel to the palaeoflow were documented (Figs. 4, 8).

Interpretation

This zone is crucial to confirm that the entire palaeosurface was covered by ripples, and the absence of this ripples in the Zone C is directly related to the generation of the tracks. The dominance of flood flows over ebb flows is also confirmed in this case. The extremely eroded ripples only preserve relict of the troughs and only preserve isolated tracks with wrinkle marks.

Ichnology

The track-bearing surface from Zone C contains at least 20 isolated tracks (see measurements in Table 1), 9 of which are elongated (length/width ratio greater than 2) including tracks 1–6, 8, 15–16 (Fig. 5). In general tracks from this zone present rounded ends and rims and have a similar orientation between them as marked with arrows in the interpretative scheme (Fig. 5B); they are parallel to the interpreted palaeochannel (Zone B) and coincide with the flood-ebb direction observed in ripple cross stratification (Figs. 4 and 5). No track overlapping was identified on the track-bearing surface. The entire area where the tracks are preserved (shadedarea in Fig. 5B) is about 3 m^2. Considering only the surface of the tracks (the total sum is about 0.64 m^2), the percentage of this surface imprinted by tracks is 21.33 %, which implies light to moderate dinosaur trampling sensu the dinoturbation index of Lockley and Conrad (1989).

The tracks are generally straight and have an approximately constant width. Track 1 is elongated, about 35.2 cm long and 16.2 cm wide, with one rounded end and the opposite end straighter. It is the closest track to the ripple-bearing surface (Fig. 5 and 6E). Track 1 presents a completely smooth and flat surface as reflected in both the photographs and the colour depth image, and the rims are more developed towards the rounded end sides. Track

2 is elongated and sinuous, about 39.2 cm long and with a maximum width of 13.4 cm close to the subrounded end. The width is almost constant along the track narrowing slightly towards the opposite, straighter end. Track 3 is elongated, straight, has a rounded end and a straighter opposite end, and is about 42.3 cm long and 18.4 cm wide. Track 3 is next to track 2 and is wider than track 2. Both tracks are parallel and present the same orientation, and the rounded end of each track extends to the same distance (Fig. 5). Track 4 is elongated, about 29.1 cm long and 11.7 cm wide, presents a subrounded asymmetrical end and a straightened opposite end. This track is charachterized by well-developed lateral rims producing lobes of variable width (maximum width: 4 cm); its subrounded end also shows a rim, about 1 cm in width. Track 5 is elongated and slightly sinuous developing narrow lateral rims; it is 37.4 cm long and exhibits a maximum width of 13.9 cm and a minimum width of 10.4 cm. Also, a shallower and narrowing posterior prolongation (12.6 cm long) of this track is recognized, as a result, the total length of track 5 could be as long as 50.5 cm. Tracks 4 and 5 are close (separated by 8 cm), and subparallel; track 4 presents an angle of 26° with respect to track 5. Track 6 is also elongated and mostly straight, but it curves at one end; it is 27.8 cm in length and 11.8 cm in width, presents an almost constant width, and one end is rounded and the opposite is not well defined. Unlike other elongated tracks that are close together such as 1, 2 and 3 on one side and 4 and 5 on the other, there are no elongated tracks in close proximity to track 6. Track 7 is wider than long, has a length of 12.2 cm and a width of 26.1 cm; it has a crescent shape, with a rounded anterior margin and the opposite one straighter and wedges towards both sides. This track presents the development of rims (about 3 cm in width) mainly on the anterior margin and in turn becomes deeper towards there. Track 7 is located just in front of track 5 and is approximately twice as wide as the latter. Track 8 is elongated, has a length of 35.5 cm and a maximum width of 16.3 cm and a minimum width of 7.7 cm; it has a subcircular shape towards the wider end but the rest of the track is rather elongated to subtriangular. This, suggests that perhaps it is the result of the superposition of two tracks. This track is completely parallel to track 4 and about 32 cm from it. Track 9 is subsquare to subrounded and is slightly longer than wide; it is 28.1 cm

long and has 20.7 cm in maximum width and 12.8 cm in minimum width. The wider end is more rounded than the opposite one, and the rim that is present along the entire perimeter of the track is more developed towards this wider end. In track 9 an acuminate mark was identified towards the right lateral margin of the wider end (Fig. 7B). Also, in this track, two levels of depth were recognized, a deeper one with a half circle shape towards the wider end and another shallower level for the rest of the track (Fig. 7C). Track 9 is next to track 8 and they are parallel to each other. Track 10 is poorly preserved and is subcircular to sub-square in shape with a length of 25.7 cm and a width of 18.1 cm, and is not parallel to tracks 8 and 9. Track 11 is also poorly preserved, one of the lateral margins is straight and the opposite has only a straight fragment and the other one widens with a circular margin; both ends are straight to subrounded. Track 11 is 20.5 cm long and 18.2 cm wide, and presents a more similar orientation to track 8 than track 10. Track 12 is the smallest track on this study surface and was recognized primarily by a recurved rim, this track is wider than long, 5.0 cm in length and 10.2 cm in width, the rest of the track presents a poorly defined margin. Track 13 is sub-square, 16.4 cm long and 12.0 cm wide, one end is straight to subrounded and the track widens slightly towards the opposite end, which is not preserved; therefore, this track was probably originally elongated. It has the same orientation as track 5 and they are almost aligned with each other, separated by about 63 cm. Track 14 is subrounded and has a similar length and width of 12.7 and 12.5 cm, respectively. Track 15 is sub-square, straight to slightly curved and is elongated, has a length of 36.2 cm and an approximately constant width, with a maximum width is 12.7 cm. Track 15 has an orientation very similar to tracks 1, 2 and 3. Track 16 is poorly preserved, has a blunt end and the opposite is not defined; it is an elongated track 31.3 cm long and 14.9 cm wide. This track has the same orientation as tracks 2 and 3 and is aligned with track 2 but separated from it by 17.2 cm. Track 17 is poorly preserved, has one rounded end and the rest of the track is incomplete; as a result it is at least 15.2 cm long and 12.5 cm wide. Track 18 is elongated with one end rounded and the other unpreserved; it is about 31.8 cm long and presents a maximum width of 18.6 cm. This track is located between tracks 4 and 16 with a similar orientation to the first one, but is

considerably wider than track 4. Track 19 is subrounded, poorly defined, with a possible length of 21.6 cm and a width of 21.3 cm. Finally, track 20 has a subrectangular shape with only one subrounded end preserved; it is 22.9 cm long and 12.8 cm wide. This track 20 presents a similar orientation to track 4.

Unlike track 1, other tracks are not as homogeneously flat and instead show slight irregularities, such as those in tracks 4 and 5, while others present more marked depth variations such as track 15 (Fig. 5A).

In Zone D some isolated crescent-shaped tracks have been documented (Fig. 8). These tracks did not develop rims and do not preserve anatomical features. Track 21 is wider than long and presents 6.5 cm in length and 11.1 cm in width. This track is breaking up a microbial mat wrinkle structure. The wrinkle structures are not preserved inside the track (Fig. 8C–F). Track 22 is wider than long, 5 cm in length and 12.3 cm in width. Track 22 displays the opposite orientation of track 21 and there are 8 cm in between the two tracks. Track 23 is wider than long, 7 cm in length, and 14 cm in width, and shows a similar orientation to track 21 and is separated from it by 44 cm.

Substrate analysis and ichnotaphonomy

In the present work, rock samples bearing wrinkle marks and fragments of rims of the tracks in Zone C were analysed under SEM. Similarly to what was observed in Zone B, filament-like microstructures were identified in the wrinkle marks. Generally, these structures consist of ensheathed forms (Fig. 9A) and they are continuous and mostly oriented parallel to the surface (Fig. 9B). Small clusters of probable coccoidal forms are also associated with the structures (Fig. 9C). On the contrary, the SEM analysis of samples from the lateral rims of the tracks (Zone C) display clear evidence of disturbance (bending and remobilization) of filaments and EPS (Fg. 9D).

Microbially induced sedimentary structures (MISS), as evidence of microbial mat formation, have been found in Precambrian to Cenozoic siliciclastic deposits in different palaeoenvironments, including tidal flat settings of Cretaceous age (Noffke *et al*. 2008 and references therein). As was previously mentioned, the presence of MISS was documented in

Zone B of the studied surface and indicates the role of microbial mats in the biostabilization of the area and the excellent preservation of invertebrate trace fossils (Fernández and Pazos 2013). Filament-like, continuous microstructures, mostly oriented parallel to the surface, but some perpendicular to the bedding plane, were found between the sand particles of the uppermost few millimetres of the surface in Zone B (Fernández and Pazos 2013, fig. 8A–B). They were interpreted as ensheathed forms of bacteria or cyanobacteria, one of the most common morphotypes of benthic cyanobacteria that formed microbial mats in ancient tidal flats (Gerdes *et al*. 2000; Schieber *et al*. 2007; Noffke 2010).

Taking into account the microtopography related to the lateral migration of a tidal channel (see Section “The track-bearing palaeosurface”) and the trace fossils and microbial mats of the studied surface, the following temporal order of mat development (summarized in 3 stages) is proposed. In a first stage (Stage 1), endobenthic microbial mats developed (identified by Fernández and Pazos 2013) with the consequent stabilization of ripples during the inundationin which the system was not completely exposed. After stabilization of the surface, horseshoe crabs produced *Kouphichnium* in Zone B (Fernández and Pazos 2013). In a second stage (Stage 2), the area was exposed and flat-topped ripples formed in Zone B. Also the ripples formed in Zone D were eroded when water level went low; microbial mats were developed at least partially as the relict wrinkle marks that are documented in ripple troughs in Zone D. The exposure is also documented by the tracks in this palaeosurface, almost flat, with the biostabilized substrate generating a slippery surface. Furthermore, microbial mats could have induced an early cementation that would directly increase the preservation potential of tracks (e.g. Marty *et al*. 2009; Carmona *et al*. 2012; Cuadrado *et al*. 2021). The trampling is another form of biogenic modification of the substrate, in this case superimposed on a microbially-induced modification. The lateral rims of the tracks with disturbance of filaments and EPS, confirm the order of development between biostabilization and bioturbation. Finally (Stage 3), microbial mats recovered, and some tracks preserve the corrugated features ascribed to wrinkle marks inside the tracks (Figs. 6C–D and 7D, F–H)

indicating an “spongy” surface, probably retaining ponded water inside that avoided desiccation cracks development.

Discussion

Producer

In this section the possible producerof the trace fossils from Zone C will be discussed considering: first, the xiphosurid producerbecause they were recognized in the same palaeosurface; then, aquatic vertebrates such as flattened fish capable of that producing elongated trace fossils, and marine reptiles; finally, terrestrial tetrapods, particularly sauropod dinosaurs.

In Zone B abundant arthropod trackways with several preservational variations were documented. As previously mentioned, these trace fossils, preserved on a biostabilized substrate, were assigned to *Kouphichnium* isp. by Fernández and Pazos (2013), and five track morphotypes were established, some of which involve pusher-leg movement. These trackways were attributed to xiphosurids, and likely produced by members of the subfamily Limulinae (Fernández and Pazos 2013). Neoichnological observations of trackways produced by modern horseshoe crabs (Limulidae Leach 1819) on different substrates (non biostabilized) such as dry subaerial sand, wet subaerial carbonate mud and very wet subaquatic carbonate mud show, that in all these cases (although in different degree of detail), appendage, prosoma and telson marks are produced (Diedrich 2011, p. 96, fig. 15). Also, xiphosurid trace fossils with prosoma drag marks remobilizing the sediment are usually associated with a tail drag mark (e.g. Fernández and Pazos 2013, pp. 19–21, figs. 3–5; Shibata and Varricchio 2020, p. 894, fig. 7). No evidence of arthropod appendage impressions or grooves that could be attributed to a telson were recognized in Zone C. It is known that the horseshoe crab prosoma is symmetrical (see Bicknell *et al*. 2021); nevertheless, some of the tracks recognized have asymmetrical rounded margins (e.g. track 4, Fig. 7). The prosoma of the producerof *Kouphichnium* trackways from Zone B was estimated by Fernández and Pazos (2013) to be about 2.5 cm wide and considering that the minimum width from the elongated tracks from Zone C is about 12 cm, the former would not

have been large enough to produce the tracks analysed in this paper. Interestingly, during the Early Cretaceous, the only two limulid body fossils recorded, *Victalimulus mcqueeni* Riek and Gill 1971 from Australia and *Crenatolimulus paluxyensis* Feldmann *et al*. 2011 from the USA, reach about 10–12 cm in width, while during the Late Cretaceous, limulids reach larger sizes, with prosomas exceeding 20 cm in width (Bicknell *et al*. 2021 and reference therein). Nevertheless, due to the bias of xiphosuran body fossil record from South America, the only evidence of a probable size was inferred from the above-mentioned *Kouphichnium* record, recognized in Zone B. Additionally, tracks of Zone C are in general flattened and although some have a rounded end, there is no evidence of scratch marks or a preservation in concave epirelief indicative of burrowing, as is the case of *Crescentichnus* Romano and Whyte 2015 and *Selenichnites* Romano and Whyte 1990 (about 1.6 cm and 1.8–2.2 cm in width, respectively) which are commonly associated with xiphosurids (Leibach *et al*. 2020 and references therein). As a result, a xiphosurid or any other similar arthropod is disregarded as the possible producer of the elongated tracks from Zone C.

Elongated and flattened trace fossils recorded at the bottom of a flooded area have been attributed to fish with relatively flat bodies and longer than wide ratios, and behavior including resting and predation with excavation (e.g. Lkebir *et al*. 2020). This excavation involves removal and accumulation of mud from the upper levels of the sediment, while resting impressions are produced through sliding on the bottom surface. In the elongated tracks of Zone C, there is no evidence of sediment being removed by excavation, but rather the displacement of sediment forming rims as a result of an impression. Also, it is unlikely that a fish would have been heavy enough to produce a resting mark deforming this biostabilized substrate. Some cartilaginous fishes with a typically dorsoventrally flattened body such as rays are capable of producing bowl-shaped feeding burrows that have been related to *Piscichnus waitemata* Gregory 1991 (see Gregory 1991; Martinell *et al*. 2001; Kotake 2007; Uchman *et al*. 2019). Although the oldest record of this ichnotaxon is from the Upper Cretaceous, an older *Piscichnus* is possible taking into account that the earliest batoids (rays and skates) are known since the Early Jurassic (Uchman *et al.* 2019 and

references therein). However these bowl-shaped burrows are completely different morphologically from the tracks documented in Zone C. On the other hand, horizontal elongated gutter-like furrows preserved in epirelief have been described as subacuatic feeding trace fossils made by marine reptiles like plesiosaurs or ichthyosaurs (Geister, 1998). These authors have documented furrows up to 60 cm wide and 9 m long and up to 30 cm deep, but they have also recognized smaller furrows, less than 20 cm wide and 15 cm deep. Most of the furrows are straight but shorter ones can be sinuous. However, these gutter-like furrows tend to deepen gradually towards one end, which is not the case of the elongated study tracks. In addition, these furrows lack rims and they are proportionally deeper than the elongated tracks from Zone C. Given that hese last tracks wereformed after a drop in water level, it is unfeasible that fish or marine reptiles could have produced them. Finally, excavations or resting tracesof these fishes and feeding grooves made by marine reptiles could not explain the crescent shape of the tracks.

The terrestrial tetrapod record from the Lower Cretaceous of the Neuquén Basin is mainly based on dinosaurs and includes: theropod and sauropod remains and tracks from fluvial deposits of the lower Valanginian Mulichinco Formation (Pino *et al*. 2020, 2021); dinosaur tracks from the Agrio Formation, comprising dinosaur tracks from marginal-marine deposits of the upper Valanginian–lower Hauterivian Pilmatué Member (Pazos *et al*. 2020); dinosaur tracks from fluvio-aeolian deposits of the middle Hauterivian Avilé Member (Heredia and Pazos 2016); non-avian theropod tracks from marginal-marine deposits of the upper Hauterivian Agua de la Mula Member (Pazos *et al*. 2012a); and sauropod remains and tracks from fluvial deposits of the Aptian–Albian Rayoso Formation (Canudo *et al*. 2017, 2018). In the Agua de la Mula Member from the Agrio Formation, occurring at stratigraphically lower levels than the study surface (see Fig. 2), large tridactyl theropod tracks assigned to cf. *Therangospodus pandemicus* and displaying a mean length and width of 34.5 cm and 23.8 cm, respectively, have been documented (Pazos *et al*. 2012a). These authors concluded that these tracks were imprinted after withdrawal of the water, when the

surface was subaerially exposed, and revealed the presence of more than one trampling episode on the same palaeosurface and fluctuations in the coastline.

The studied surface shows evidence of microbial mat development (see Section "Substrate analysis and ichnotaphonomy"), which have made the surface slippery. As a result, elongated tracks from Zone C may represent slips on an slippery biostabilized surface. Taking into account that the tracks are almost subparallel and indicate the same direction of displacement, according to the rounded edges, and that they do not overlap each other in any case, it is possible to infer that several producerspassed in the same direction parallel to the channel of the Zone B. It is also possible to assume that the producers must have been heavy enough to imprint the tracks and deform this biostabilized substrate. However, at the same time, the properties of the substrate constrained the preservation of defined anatomical features, unlike other tetrapod slipping track records without a biostabilized substrate (e.g. Wings *et al*. 2007; Díaz-Martínez *et al*. 2020). In the studied track-bearing surface, some of the elongated parallel tracks could belong to the same pair of limbs (manus or pes) given their proximity and that they extend almost to the same point (e.g. tracks 2 and 3 or tracks 4 and 5). Some short tracks associated with elongated ones, as is the case of the crescentic-shaped track 7 (Fig. 7A, D, E) which is located just in front of elongated track 5, could represent a manus track of the same producer while stopping. The latter is consistent with the morphology of the track with a non-uniform depth (unlike the elongated flattened tracks), which deepens towards one end and where a prominent rim has developed. Track 9 has an asymmetrical shape that is longer than wide and subtriangular with rounded ends, and the curved wider extreme presents a laterally acuminate mark (Fig. 7B). This probably represents the impression of one claw oriented laterally. It is also observed that it is deeper towards the wider end (interpreted as the track anterior side; Fig. 7C). In the Rayoso Formation of the overlying Bajada del Agrio Group (see Fig. 1B), Canudo *et al.* (2017) have documented small sauropod tracks between 17 and 23 cm wide, and track 9 studied here falls within this size range. Considering all these track features, track 9 is interpreted as a sauropod right pes track. It has been

proposed that the claws present in sauropods would act as traction devices, preventing the foot from sliding backwards during support and propulsion (Bonnan 2005). Among the smallest known sauropod manus and pes tracks are those documented by Lockley *et al*. (2018) from the Lower Cretaceous Jingchuan Formation of China. The length and width of these sauropod manus tracks are 5.0 and 6.0 cm, respectively, and the length and width of pes tracks are 11.5 and 7.5 cm, respectively. These authors also recorded small sauropod pes tracks with a width range of 7.5–24.5 cm, while the tracks from the present study of the Agrio Formation range from 10.2–21.3 cm in width (excluding track 7), thus falling within this range. The fact that some elongated tracks are sinuous is probably the result of slipping by a tetrapod; possessing legs that are mobile with respect to its center of mass, sometimes these legs tend to move inward and outward relative to the midline describing sinuous trajectories when slipping. Sinuous and flattened tracks have been observed in the slips left by some juvenile elephants when slipping down the bank of a muddy river (see videos from ElephantVoices.org). Considering the substrate properties analysed (involving a biostabilized substrate with slippery conditions), the track size and depth, track morphology and orientation, it is concluded that Zone C was a dinosaur trampling area, probably produced by small sauropods. The different sizes and shapes of the tracks suggest that, if they were produced by the same type of producer, for instance the same sauropod taxon, there were different age groups involved.

Palaeolandscape

The integration of the interpreted zones, demonstrates sedimentological, ichnological and peleocological differences in a short distance on the same palaeosurface. The evidence of tidal flows in the locality was early documented by Pazos *et al.* (2012a) particulary by carabonatic shoals with reactivation surfaces, potamidid gastropods with encrusted bryozoans (Taylor *et al.* 2009) recorded at both sides of an anticline (Rayoso). The documentation of tidal flows in this area of the basin was explained as the evidence of a complete tidal influenced setting on the whole eastern side of the basin for the uppermost part of the Agrio Formation showing not differences in very distant parts of the basin (e.g.

Fernández and Pazos, 2012). Regardless of the facies trend in the underlying sequences by Pazos *et al.* (2020) and even in the subsurface correlatable levels (Pazos *et al.* 2021).

The analysed palaeosurface permits to recognise a complex history probably involving several tidal cycles, also considering that microbial mats, as mentioned before, requires at least several days for its development. The channel is interpreted as a tidal channel, more precisely a tidal creek. Any evidence of a permanent fluvial discharge is disregarded as the preserved ripples inside show almost a complete desiccation, and any evidence of a permanent fluvial discharge (ebb directed) is absent. The heterolithic nature observed in the lateral accretion is compatible with the migration of a point bar of tidal origin rather a fluvial one (e.g. Hovikoski *et al*. 2007). Moreover, the orthogonal palaeondicators of the lateral accretion structure and ripples confirms the origin of such structure and sedimentary context. The palaeosurface records a position in the upper intertidal area, and documents a different level that the underlying interval with carbonate polygon cracks. The cooccurring invertebrate and vertebrate trace fossils inside and laterally to the channel is a spectacular opportunity to reconstruct a palaeolandscape and a window to the ecology of palaeotidal flats very unusually observed in the geological record.

Conclusions

The analysis of the study surface containing several elongated and other crescent-shaped tracks and those trace fossils described by Fernández and Pazos (2013) was indicative of a local palaeotopography related to a tidal-dominated depositional system. This palaeosurface shows palaeotopographic differences over a short distance. This lateral variability observed in the field was analysed and four zones were defined. Zone A shows several carbonate levels with cracked microbial mats and records successive flooding and desiccation events. Zone B consists of an asymmetrical depression interpreted as a tidal channel that recorded rippled deposits generated during the flood tide. Zone C is the lateral continuation of the inclined surface of the channel. It is an almost flat area and bears the tracks studied here. Zone D includes a depressed area and also the most distal to Zone A,

where eroded ripples and wrinkle marks are preserved. A genetic order between mat development and bioturbation of the palaeosurface was recognized. In a first stage (Stage 1), the stabilization of ripples generated into the channel during the flood tide took place; there, horseshoe crabs produced *Kouphichnium* in Zone B (Fernández and Pazos 2013). In a second stage (Stage 2) the surface exposure close to the channel is identified by the track formation with the biostabilized substrate generating a slippery surface in Zone C. Scanning electron microscope (SEM) analysis of the rims of the tracks indicates that the microbial filaments and EPS were disturbed by the trampling. In Zone D ripples were eroded as a consequence of an ebb current and microbial mats were developed (evidenced by wrinkle marks). Finally (Stage 3), microbial mats recovered, and some tracks preserve wrinkle marks on the inside indicating an “spongy” surface, probably retaining ponded water. Considering the substrate properties and track features analysed, such as morphology, size, depth, and the parallel orientation of the tracks to the channel margin, it is concluded that the tracks were produced by dinosaurs, probably small sauropods, trampling on a slippery surface and moving parallel to the channel margin.

Acknowledgments

We sincerely thank reviewer Brian F. Platt and the other anonymous reviewer for their constructive comments and suggestions that improved the manuscript. This research was financially supported by the Consejo Nacional de Investigaciones Científicas y Técnicas, Argentina (PIP CONICET 2016–2020), and Universidad de Buenos Aires, Argentina (UBACyT 2016–2019) to Pablo J. Pazos. This is contribution R-398 of the Instituto de Estudios Andinos Don Pablo Groeber.

References

Aguirre-Urreta, B., Schmitz, M., Lescano, M., Tunik,M., Rawson, P.F., Concheyro, A., Buhler, M. and Ramos, V.A. 2017. A high precision U-Pb radioisotopic age for the Agrio Formation, Neuquén Basin, Argentina: implications for the chronology of the Hauterivian Stage. *Cretaceous Research*, **75**, 193–204. https://doi.org/10.1016/j.cretres.2017.03.027

Aguirre-Urreta, B., Martinez, M., Schmitz, M., Lescano, M., Omarini, J., Tunik, M., Kuhnert, H., Concheyro, A., Rawson, P.F., Ramos, V.A., Reboulet, S., Noclin, N., Frederichs, T., Nickl, A.L. and Pälike, H. 2019. Interhemispheric radio-astrochronological calibration of the time scales from the Andean and the Tethyan areas in the Valanginian–Hauterivian (Early Cretaceous). *Gondwana Research*, **70**, 104–132. https://doi.org/10.1016/j.gr.2019.01.006

Andrada, A.M., Bressan, G.S. and Lazo, D.G. 2020. Taphonomy of decapod-bearing concretions and their associated trace fossils from the Agrio Formation (Lower Cretaceous, Neuquén Basin), with palaeobiological implications for axiid shrimps. *Revista de la Asociación Geológica Argentina*, **77**, 366–383.

Archuby, F.M. and Fürsich, F.T., 2010. Facies analysis of a higly cyclic sedimentary unit: the Late Hauterivian to Early Barremian Agua de la Mula Member of the Agrio Formation, Neuquén Basin, Argentina. *Beringeria*, **41**, 77–127.

Bicknell, R.D., Błażejowski, B., Wings, O., Hitij, T. and Botton, M.L. 2021. Critical re-evaluation of Limulidae uncovers limited *Limulus* diversity. *Papers in Palaeontology*, 1–3 2.https://doi.org/10.1002/spp2.1352

Bonnan, M.F. 2005. Pes anatomy in sauropod dinosaurs: implications for functional morphology, evolution, and phylogeny. In: Tidwell, V., Carpenter, K. (eds.), *Thunder-Lizards*. Indiana University Press, Bloomington, 346–380.

Bose, S. and Chafetz, H.S. 2009. Topographic control on distribution of modern microbially induced sedimentary structures (MISS): a case study from Texas coast. *Sedimentary Geology*, **213**, 136–149. https://doi.org/10.1016/j.sedgeo.2008.11.009

Bradley, G.M., Redfern, J., Hodgetts, D., George, A.D. and Wach, G.D. 2018. The applicability of modern tidal analogues to pre-vegetation paralic depositional models. *Sedimentology*, **65**, 2171–2201. https://doi.org/10.1111/sed.12461

Canudo, J.I., Garrido, A., Carballido, J.L., Castanera, D. and Salgado, L. 2017. Icnitas de dinosaurios saurópodos en la Formación Rayoso (Cuenca Neuquina, Albiense, Argentina). *Geogaceta*, **61**, 43–46.

Canudo, J.I., Carballido, J.L., Garrido, A. and Salgado, L. 2018. A new rebbachisaurid sauropod from the Aptian–Albian, Lower Cretaceous Rayoso Formation, Neuquén, Argentina. *Acta Palaeontologica Polonica*, **63**, 679–691. https://doi.org/10.4202/app.00524.2018

Carmona, N., Bournod, C., Ponce, J.J. and Cuadrado, D. 2012. The role of microbial mats in the preservation of bird footprints: A case study from the mesotidal Bahia Blanca estuary (Argentina). In: Noffke, N., Chafetz, H.S. (eds.), *Microbial Mats in Siliciclastic Depositional Systems Through Time: Tulsa, SEPM Special Publication*, **101**, 37–45. https://doi.org/10.2110/sepmsp.101.037

Cichowolski, M., Pazos, P.J., Tunik, M.A. and Aguirre-Urreta, M.B. 2012. An exceptional storm accumulation of nautilids in the Lower Cretaceous of the Neuquén Basin, Argentina. *Lethaia*, **45**, 121–138. https://doi.org/10.1111/j.1502-3931.2011.00271.x

Comerio, M., Fernández, D.E. and Pazos, P.J. 2018. Sedimentological and ichnological characterization of muddy storm related deposits: The upper Hauterivian ramp of the Agrio Formation in the Neuquén Basin, Argentina. *Cretaceous Research*, **85**, 78–94. https://doi.org/10.1016/j.cretres.2017.11.024

Cuadrado, D.G., Maisano, L. and Quijada, I.E. 2021. Role of microbial mats and high sedimentation rates in the early burial and preservation of footprints in a siliciclastic tidal flat. *Journal of Sedimentary Research*, **91**, 479–494. https://doi.org/10.2110/jsr.2020.149

Dai, H., Xing, L., Marty, D., Zhang, J., Persons IV, W.S., Hu, H. and Wang, F. 2015. Microbially-induced sedimentary wrinkle structures and possible impact of microbial mats for the enhanced preservation of dinosaur tracks from the Lower Cretaceous Jiaguan

Formation near Qijiang (Chongqing, China). *Cretaceous Research*, **53**, 98–109. https://doi.org/10.1016/j.cretres.2014.10.012

de Souza Carvalho, I., Borghi, L. and Leonardi, G. 2013. Preservation of dinosaur tracks induced by microbial mats in the Sousa Basin (Lower Cretaceous), Brazil. *Cretaceous Research*, **44**, 112–121. https://doi.org/10.1016/j.cretres.2013.04.004

Díaz-Martínez, I., Pérez-Lorente, F., Canudo, J.I. and Pereda-Suberbiola, X. 2009. Causas de la variabilidad en icnitas de dinosaurios y su aplicación en icnotaxonomía. Actas de las IV Jornadas Internacionales sobre Paleontología de Dinosaurios y su Entorno. Salas de los Infantes, Burgos, 207–220.

Díaz-Martínez, I., Suarez-Hernando, O., Larrasoaña, J. C., Martínez-García, B. M., Baceta, J.I. and Murelaga, X. 2020. Multi-aged social behaviour based on artiodactyl tracks in an early Miocene palustrine wetland (Ebro Basin, Spain). *Scientific reports*, **10**, 1–16. https://doi.org/10.1038/s41598-020-57438-4

Diedrich, C.G. 2011. Middle Triassic horseshoe crab reproduction areas on intertidal flats of Europe with evidence of predation by archosaurs. *Biological Journal of the Linnean Society*, 103, 76–105. https://doi.org/10.1111/j.1095-8312.2011.01635.x

ElephantVoices.org. Elephant sliding down the river bank, www.youtube.com/watch?v=MwvA4_kVTnc

Emmons, E. 1844. The Taconic System, Based on observations in New York, Massachusetts, Maine, Vermont and Rhode Island. Albany, Caroll and Cook, 68 pp.

Falkingham, P.L. 2012. Acquisition of high resolution three dimensional models using free, open-source, photogrammetric software. *Palaeontologia Electronica*, **15**, 1–15. https://doi.org/10.26879/264

Falkingham, P.L. 2014. Interpreting ecology and behaviour from the vertebrate fossil track record. *Jorunal of Zoology*. **292**, 222–228. https://doi.org/10.1111/jzo.12110

Feldmann, R.M., Schweitzer, C.E., Dattilo, B. and Farlow, J.O. 2011. Remarkable preservation of a new genus and species of limuline horseshoe crab from the Cretaceous

of Texas, USA. *Palaeontology*, **54**, 1337–1346. https://doi.org/10.1111/j.1475-4983.2011.01103.x

Fennell, L.M., Naipauer, M., Borghi, P., Sagripanti, L., Pimentel, M. and Folguera, A. 2020. Early Jurassic intraplate extension in west-central Argentina constrained by U-Pb SHRIMP dating: Implications for the opening of the Neuquén basin. *Gondwana Research*, **87**, 278–302. https://doi.org/10.1016/j.gr.2020.06.017

Fernández, D.E. 2013. Icnología de facies marino-marginales en el Cretácico Inferior de la Cuenca Neuquina (Doctoral dissertation, Phd thesis, Universidad de Buenos Aires (unpublished), 440 p., Buenos Aires).

Fernández, D.E. and Pazos, P.J. 2012. Ichnology of marginal marine facies of the Agrio Formation (Lower Cretaceous, Neuquén Basin, Argentina) at its type locality. *Ameghiniana*, **49**, 505–524. https://doi.org/10.5710/AMGH.23.7.2012.439

Fernández, D.E. and Pazos, P.J. 2013. Xiphosurid trackways in a Lower Cretaceous tidal flat in Patagonia: palaeoecological implications and the involvement of microbial mats in trace-fossil preservation. *Palaeogeography, Palaeoclimatology, Palaeoecology*, **375**, 16–29. https://doi.org/10.1016/j.palaeo.2013.02.008

Fernández, D.E. and Pazos, P.J. 2015. Ichnological research in Lower Cretaceous marginal-marine facies from Patagonia: outcrop studies, SEM examinations and paleontological/sedimentological integration. *Neues Jahrbuch für Geologie und Paläontologie-Abhandlungen*, **277**, 177–188. https://doi.org/10.1127/njgpa/2015/0500

Fernández, D.E., Pazos, P.J. and Aguirre-Urreta, M.B. 2010. *Protovirgularia dichotoma—Protovirgularia rugosa*: an example of a compound trace fossil from the Lower Cretaceous (Agrio Formation) of the Neuquén Basin, Argentina. *Ichnos*, **17**, 40–47. https://doi.org/10.1080/10420941003659436

Fernández, D.E., Comerio, M. and Pazos, P.J. 2018. *Nereites* in Lower Cretaceous marginal-marine facies from Patagonia: Ichnotaxonomic and ethological implications. *Cretaceous Research*, **81**, 51–63. https://doi.org/10.1016/j.cretres.2017.09.002

Fernández, D.E., Comerio, M., Giachetti, L.M., Pazos, P.J. and Wetzel, A. 2019. Asteroid trace fossils from Lower Cretaceous shallow-to marginal-marine deposits in Patagonia. *Cretaceous Research*, **93**, 120–128. https://doi.org/10.1016/j.cretres.2018.09.010

Geister, J. 1998. Lebenspuren von Meersaurien und ihren Beutetieren im mittleren Jura (Callovien) von Liesberg. *Facies*, **39**, 105–124. https://doi.org/10.1007/BF02537013

Giachetti, L.M., Fernández, D.E. and Comerio, M. 2020. Analysis of *Asteriacites* von Schlotheim 1820 from Mulichinco Formation (Lower Cretaceous, Neuquén Basin) and ichnotaxonomic implications. *Revista de la Asociación Geológica Argentina*, **77**, 384–401.

Gregory, M.R. 1991, New trace fossils from the Miocene of Northland, New Zealand: *Rorschachichnus amoeba* and *Piscichnus Waitemata*. *Ichnos*, **1**, 195–205. https://doi.org/10.1080/10420949109386352

Groeber, P. 1946. Observaciones geológicas a lo largo del meridiano 70.1. Hoja Chos Malal. *Revista de la Asociación Geológica Argentina*, **1**, 177–208.

Guler, M.V., Lazo, D.G., Pazos, P.J., Borel, C.M., Ottone, E.G., Tyson, R.V., Cesaretti, N. and Aguirre-Urreta, M.B. 2013. Palynofacies analysis and palynology of the Agua de la Mula Member (Agrio Formation) in a sequence stratigraphy framework, Lower Cretaceous, Neuquén Basin, Argentina. *Cretaceous Research*, **41**, 65–81. https://doi.org/10.1016/j.cretres.2012.10.006

Heredia, A.M. and Pazos, P.J. 2016. The oldest dinosaur tracks record in the Neuquén Basin from a fluvio-aeolian Hauterivian forced regressive wedge (Avilé Member), Agrio Formation, Patagonia, Argentina. 4th International Congress on Ichnology (ICHNIA), Idanha-a-Nova, Portugal, abstract book, pp. 102–103.

Heredia, A.M., Pazos, P.J., Fernández, D.E. and Comerio, M. 2018. Las huellas de dinosaurios como evidencia de exposición subaérea del Miembro Pilmatué de la Formación Agrio (Cretácico Inferior) de la Cuenca Neuquina. XXXII Jornadas Argentinas de Paleontología de Vertebrados, Corrientes, Argentina. *Suplemento Resúmenes de la Publicación Electrónica de la Asociación Paleontológica Argentina*, **19**, R 21. https://doi.org/10.571/PEAPA.15.04.2019.295

Heredia, A.M., Díaz-Martínez, I., Pazos, P.J., Comerio, M. and Fernández, D.E. 2020. Gregarious behaviour among non-avian theropods inferred from trackways: A case study from the Cretaceous (Cenomanian) Candeleros Formation of Patagonia, Argentina. *Palaeogeography, Palaeoclimatology, Palaeoecology*, **538**, 109480. https://doi.org/10.1016/j.palaeo.2019.109480

Hitchcock, E., 1858. Ichnology of New England. A Report on the Sandstone of the Connecticut Valley, Especially Its Fossil Footmarks. W. White, Boston 220 pp.

Hovikoski, J., Räsänen, M., Gingras, M., Ranzi, A. and Melo, J. 2008. Tidal and seasonal controls in the formation of Late Miocene inclined heterolithic stratification deposits, western Amazonian foreland basin. *Sedimentology*, **55**, 499–530. https://doi.org/10.1111/j.1365-3091.2007.00907.x

Howell, J.A., Schwarz, E., Spalletti, L.A. and Veiga, G.D. 2005. The Neuquén basin: an overview. *Geological Society, London, Special Publications*, **252**, 1–14. https://doi.org/10.1144/GSL.SP.2005.252.01.01

Kotake, N. 2007. *Macaronichnus* isp. associated with *Piscichnus waitemata* in the Miocene of Yonaguni-jima Island, Southwest Japan. In: Miller III, W. (ed.), *Trace Fossils: Concepts, Problems, Prospects*, Elsevier, Amsterdam, 492–501. https://doi.org/10.1016/B978-044452949-7/50156-X

Lazo, D.G. and Damborenea, S.E. 2011. Barremian bivalves from the Huitrín Formation, west-central Argentina: taxonomy and paleoecology of a restricted marine association. *Journal of Paleontology*, **85**, 719–743. https://doi.org/10.1144/GSL.SP.2005.252.01.15

Lazo, D.G., Cichowolski, M., Rodríguez, D.L. and Aguirre-Urreta, M.B. 2005. Lithofacies, palaeoecology and palaeoenvironments of the Agrio Formation, Lower Cretaceous of the Neuquén Basin, Argentina. *Geological Society, London, Special Publications*, **252**, 295–315.

Leach, W. 1819. Entomostraca, Dictionnaire des Sciences Naturelles: Paris, Levrault and Schoell, 537 p.

Leanza, H.A., Hugo, C.A. and Repol, D. 2001. Hoja geológica 3969-I, Zapala, provincia del Neuquén. Instituto de Geología y Recursos Minerales. Servicio Geológico Minero Argentino, Boletín, **275**, 128 p. Buenos Aires

Legarreta, L. 2002. Eventos de desecación en la Cuenca Neuquina: Depósitos continentales y distribución de hidrocarburos. In: V Congreso de Exploración y Desarrollo de Hidrocarburos. Tremp, Spain. Technical works on CD.

Legarreta, L. and Gulisano, C.A. 1989. Análisis estratigráfico secuencial de la Cuenca Neuquina (Triásico Superior–Terciario Inferior). In: *Cuencas sedimentarias argentinas*, San Miguel de Tucumán, Universidad Nacional de Tucumán, **6**, 221–243.

Legarreta, L. and Uliana, M.A. 1991. Jurassic–Cretaceous marine oscillations and geometry of back-arc basin fill, central Argentine Andes. *Special Publications international Association in Sedimentology*, **12**, 429–450.

Legarreta, L. and Uliana, M.A., 1999. El Jurásico y Cretácico de la Cordillera Pricipal y la Cuenca Neuquina. Facies Sedimentarias. In: Caminos, R. (ed.) *Geología Argentina*, Servicio Nacional Minero Geológico, Anales 29, 339–416, Buenos Aires.

Leibach, W.W., Rose, N., Bader, K., Mohr, L.J., Super, K. and Kimmig, J. 2020. Horseshoe crab trace fossils and associated ichnofauna of the Pony Creek Shale Lagerstätte, Upper Pennsylvanian, Kansas, USA. *Ichnos*, **28**, 34–45. https://doi.org/10.1080/10420940.2020.1811268

Lkebir, N., Masrour, M., Torices, A. and Pérez-Lorente, F. 2020. Cubichnia and Praedichnia in fossil ichnites of a flat fish from the Lower Cretaceous Talmest palaeoichnological site, Western High Atlas (Morocco). *Ichnos*, **28**, 60–71. https://doi.org/10.1080/10420940.2020.1835661

Lockley, M.G. and Conrad, K. 1989. The paleoenvironmental context, preservation and paleoecological significance of dinosaur tracksites in the western USA. In: Gillette, D.D., Lockley, M.G. (eds.) *Dinosaur Tracks and Traces*. Cambridge University Press, Cambridge, 121–134.

Lockley, M.G., Li, J., Xing, L., Guo, B. and Matsukawa, M. 2018. Large theropod and small sauropod trackmakers from the Lower Cretaceous Jingchuan Formation, Inner Mongolia, China. *Cretaceous Research*, **92**, 150–167. https://doi.org/10.1016/j.cretres.2018.07.007

Manceda, R. and Figueroa, D. 1995. Inversion of the Mesozoic Neuquén rift in the Malargüe fold and thrust belt, Mendoza, Argentina. In: Tankard, A.J., Suárez, R., Welsink, H.J. (eds.), *Petroleum basins of South America, AAPG Memoir*, **62**, 369–382. https://doi.org/10.1306/M62593C18

Manning, P.L. 2004. A new approach to the analysis and interpretation of tracks: examples from the dinosauria. In: McIlroy, D. (Ed.), The Application of Ichnology to Palaeoenvironmental and Stratigraphic Analysis. *Geological Society, London, Special Publications*, **228**, 93–123. https://doi.org/10.1144/GSL.SP.2004.228.01.06

Martinell, J., De Gibert, J.M., Domènech, R., Ekdale, A.A. and Steen, P.P. 2001. Cretaceous ray traces?: an alternative interpretation for the alleged dinosaur tracks of La Posa, Isona, NE Spain. *Palaios*, **16**, 409–416. https://doi.org/10.1669/0883-1351(2001)016<0409:CRTAAI>2.0.CO;2

Marty, D., Strasser, A. and Meyer, C.A. 2009. Formation and taphonomy of human footprints in microbial mats of present-day tidal-flat environments: implications for the study of fossil footprints. *Ichnos*, **6**, 127–142. https://doi.org/10.1080/10420940802471027

Milàn, J. and Bromley, R.G. 2008. The impact of sediment consistency on track and undertrack morphology: experiments with emu tracks in layered cement. *Ichnos*, **15**, 19–27. https://doi.org/10.1080/10420940600864712

Naipauer, M. and Ramos, V.A. 2016. Changes in Source Areas at Neuquén Basin: Mesozoic Evolution and Tectonic Setting Based on U–Pb Ages on Zircons. In: *Growth of the Southern Andes*. Springer, Cham, pp. 33–61. https://doi.org/10.1007/978-3-319-23060-3_3

Noffke, N. 2010. Geobiology: microbial mats in sandy deposits from the Archean era to today. Springer-Verlag, Berlin. https://doi.org/10.1007/978-3-642-12772-4

Noffke, N., Gerdes, G., Klenke, T. and Krumbein, W.E. 2001. Microbially induced sedimentary structures: a new category within the classification of primary sedimentary structures. *Journal of Sedimentary Research*, **71**, 649–656. https://doi.org/10.1306/2DC4095D-0E47-11D7-8643000102C1865D

Noffke, N., Beukes, N., Bower, D., Hazen, R.M. and Swift, D.J.P. 2008. An actualistic perspective into Archean worlds–(cyano-) bacterially induced sedimentary structures in the siliciclastic Nhlazatse Section, 2.9 Ga Pongola Supergroup, South Africa. *Geobiology*, **6**, 5–20. https://doi.org/10.1111/j.1472-4669.2007.00118.x

Nopcsa, F. 1923. Die Familien der Reptilien. Fortschritte der Geologie und Palaeontologie, **2**, 1–210.

Paik, I.S., Kim, H.J., Lee, H. and Kim, S. 2017. A large and distinct skin impression on the cast of a sauropod dinosaur footprint from Early Cretaceous floodplain deposits, Korea. *Scientific reports*, **7**, 16339. https://doi.org/10.1038/s41598-017-16576-y

Pazos, P. 2009. Síntesis icnológica de unidades mesozoicas marinas de la Cuenca Neuquina, nuevos datos y perspectivas. *Revista de la Asociación Geológica Argentina*, **65**, 362–372.

Pazos, P. 2011. Icnología de Neuquén. Relatorio del XVIII Congreso Geológico Argentino, pp. 591–600.

Pazos, P.J. and Fernández, D.E. 2010. Three-dimensionally integrated trace fossils from shallow-marine deposits in the Lower Cretaceous of the Neuquén Basin (Argentina): *Hillichnus agrioensis* isp. nov. *Acta Geologica Polonica*, **60**, 105–118.

Pazos, P.J., Lazo, D.G., Tunik, M.A., Marsicano, C.A., Fernández, D.E. and Aguirre-Urreta, M.B. 2012a. Paleoenvironmental framework of dinosaur track-sites and other ichnofossils in Early Cretaceous mixed siliciclastic-carbonate deposits in the Neuquén Basin, northern Patagonia (Argentina). *Gondwana Research*, **22**, 1125–1140. https://doi.org/10.1016/j.gr.2012.02.003

Pazos, P.J., Fernández, D.E., Comerio, M. and Ottone, G.E. 2012b. Ichnology of an Intertidal Palaeosurface: The Record of Tidal Water Fluctuations, Palaeotopography,

Microbial Mat Variability and Trace Fossil Distribution in the Lower Cretaceous of Patagonia, Argentina. 3rd International Congress on Ichnology (ICHNIA), St John's, Newfoundland, Canada, abstract book, pp. 74.

Pazos, P.J., Comerio, M., Fernández, D.E., Gutiérrez, C., González Estebenet, M.C. and Heredia, A.M. 2020. Sedimentology and sequence stratigraphy of the Agrio Formation (Late Valanginian–earliest Barremian) and the closure of the Mendoza Group to the north of the Huincul High. In: *Opening and closure of the Neuquén Basin in the Southern Andes*. Kietzmann, D., Folguera, A. (eds.). Springer Earth System Science. Springer, Cham, pp. 237–265. https://doi.org/10.1007/978-3-030-29680-3_10

Pino, D., Gómez, R., Zalazar, M., Díaz-Martínez, I., Tunik, M. and Coria, R.A. 2020. Nuevas asociaciones de huellas de dinosaurios en facies continentales de la Formación Mulichinco (Valanginiano Temprano), Cuenca Neuquina, Argentina. Segundas Jornadas de Paleovertebrados de la Cuenca Neuquina, Libro de Resúmenes, *Publicación Electrónica de la Asociación Paleontológica Argentina*, **20**, R15. https://doi.org/10.5710/PEAPA.07.07.2020.329

Pino, D.A., Coria, R.A., Díaz-Martínez, I. and Tunik, M.A. 2021. An accumulation of dinosaur remains in fluvial deposits of Mulichinco Formation (lower Valanginian, Neuquén Basin), Patagonia, Argentina: Taphonomic and paleoenvironmental inferences. *Journal of South American Earth Sciences*, **105**, 102979. https://doi.org/10.1016/j.jsames.2020.102979

Platt, B.F., Hasiotis, S.T., Hirmas and D.R. 2012. Empirical determination of physical controls on megafaunal footprint formation through neoichnological experiments with elephants. *Palaios*, **27**, 725–737. https://doi.org/10.2110/palo.2012.p12-006r

Riek, E.F. and Gill, E.D. 1971. A new xiphosuran genus from Lower Cretaceous freshwater sediments at Koonwarra, Victoria, Australia. *Palaeontology*, **14**, 206–210.

Romano, M., and Whyte, M.A. 1990. *Selenichnites*, a new name for the ichnogenus *Selenichnus* Romano and Whyte, 1987. *Proceedings of the Yorkshire Geological Society*, **48**, 221–221. https://doi.org/10.1144/pygs.48.2.221

Romano, M., and Whyte, M.A. 2015. A review of the trace fossil *Selenichnites*. *Proceedings of the Yorkshire Geological Society*, **60**, 275–288. https://doi.org/10.1144/pygs2015-357

Schieber, J., Bose, B.K., Eriksson, P.G., Banerjee, S., Altermann, W. and Catuneau, O. (eds.) 2007. *Atlas of microbial mat features preserved within the clastic rock record*. Elsevier, Amsterdam, 324p.

Schwarz, E., Veiga, G.D., Álvarez Trentini, G., Isla, M.F. and Spalletti, L.A. 2018. Expanding the spectrum of shallow-marine, mixed carbonate–siliciclastic systems: Processes, facies distribution and depositional controls of a siliciclastic-dominated example. *Sedimentology*, **65**, 1558–1589. https://doi.org/10.1111/sed.12438

Shibata, M. and Varricchio, D.J. 2020. Horseshoe crab trace fossils from the Upper Cretaceous Two Medicine Formation of Montana, USA, and a brief review of the xiphosurid ichnological record. *Journal of Paleontology*, **94**, 887–905. https://doi.org/10.1017/jpa.2020.16

Spalletti, L.A., Poiré, D.G., Schwarz, E. and Veiga, G.D. 2001. Sedimentologic and sequence stratigraphic model of a Neocomian marine carbonate–siliciclastic ramp: Neuquén Basin, Argentina. *Journal of South American Earth Sciences*, **14**, 609–624. https://doi.org/10.1016/S0895-9811(01)00039-6

Tunik, M.A., Pazos, P.J., Impiccini, A., Lazo, D. and Aguirre-Urreta, M.B. 2009. Dolomitized tidal cycles in the Agua de la Mula Member of the Agrio Formation (Early Cretaceous), Neuquén Basin, Argentina. *Latin American Journal of Basin Analysis*, **16**, 29–43.

Taylor, P.D., Lazo, D.G. and Aguirre-Urreta, M.B. 2009. Lower Cretaceous bryozoans from Argentina: a 'by-catch' fauna from the Agrio Formation (Neuquén Basin). *Cretaceous Research*, **30**, 193–203. https://doi.org/10.1016/j.cretres.2008.07.003

Uchman, A., Torres, P., Johnson, M.E., Berning, B., Ramalho, R.S., Rebelo, A.C., Melo, C.S., Baptista, L., Madeira, P., Cordeiro, R. and Avila, S.P. 2018. Feeding traces of recent ray fish and occurrences of the trace fossil Piscichnus waitemata from the Pliocene of Santa Maria Island, Azores (Northeast Atlantic). *Palaios*, **33**, 361–375. https://doi.org/10.2110/palo.2018.027

Veiga, G.D., Spalletti, L.A. and Flint, S.S. 2007. Anatomy of a fluvial lowstand wedge: the Avilé Member of the Agrio Formation (Hauterivian) in central Neuquén Basin (northwest Neuquén province), Argentina. In: Nichols, G., Williams, E., Paola, C. (eds.). *Sedimentary Processes, Environments and Basins*. A tribute to Peter Friend. International Association of Sedimentologists, Special Publication, **38**, 341–365. https://doi.org/10.1002/9781444304411.ch16

Vergani, G.D., Tankard, A.J., Belotti, J. and Welsink, H.J. 1995. Tectonic evolution and paleogeography of the Neuquén Basin, Argentina. In: Tankard, A.J., Suárez, R., Welsink, H.J. (eds.), *Petroleum basins of South America*, American Association of Petroleum Geologists: Memoir, **62**, 383–402. https://doi.org/10.1306/M62593C19

Weaver, C.E. 1931. Paleontology of the Jurassic and Cretaceous of West Central Argentina. Memoir of the University of Washington, **1**, 1–469.

Wings, O., Schellhorn, R., Mallison, H., Thuy, B., Wu, W. and Sun, G. 2007. The first dinosaur tracksite from Xinjiang, NW China (Middle Jurassic Sanjianfang Formation, Turpan Basin)—a preliminary report. *Global Geology*, **10**, 113–129.

Xing, L., Lockley, M.G., Tang, D., Klein, H., Peng, G., Ye, Y. and Hao, B. 2019. Early Jurassic basal sauropodomorpha dominated tracks from Guizhou, China: Morphology, ethology, and paleoenvironment. *Geoscience Frontiers*, **10**, 229–240. https://doi.org/10.1016/j.gsf.2018.06.001

Figure Captions

Fig.1. (**A**) General map and facies distribution during the late Hauterivian in the Neuquén Basin (modified from Legarreta and Uliana 1991, 1999). The study area (Cerro Rayoso) is marked with a white star. (**B**) Upper Jurassic–Palaeogene lithostratigraphy column of the Neuquén Basin (Modified from Howell *et al*. 2005). The Agua de la Mula Member of the Agrio Formation is indicated by a red arrow. U–Pb, CA-ID-TIMS zircon ages obtained from tuff levels in the Pilmatué (Aguirre-Urreta *et al*. 2017) and the Agua de la Mula members (Aguirre-Urreta *et al*. 2019) are shown.

Fig. 2. Logged section of the upper part of the Agua de la Mula Member (Agrio Formation) in the Cerro Rayoso locality. The studied surface is indicated by a white-filled arrow while the black-filled arrows indicate the directions of the palaeocurrents (modified from Fernández 2013 and Fernández and Pazos 2013). Cl, claystone; Sl, siltstone; Md, mudstone; fS, fine sandstone; mS, medium sandstone; cS, coarse sandstone; C, conglomerate; Pkst, packstone; Grst, grainstone.

Fig. 3. (**A**) Carbonate desiccation polygons from Zone A. Rock pick: 33 cm. (**B**) False-colour depth image of the transition between Zone B and Zone C, including the ripple- and track-bearing surface, respectively. White arrow indicates the flood flow direction. Scale bar: 30 cm. (**C**) Photograph in perspective of both Zone B and Zone C. White arrow indicates the flood flow direction. (**D**) Laterally extended lines below the eroded ripple tops from Zone B indicated by arrow heads. Flood flow direction indicated by white arrow. Scale bar: 14 cm. (**E**) Parallel lines indicating the water level position in a modern tidal flat such as the Mont Saint Michael, France. Scale bar: 10 cm.(F) Wrinkle marks preserved inside one of the several tracks from the Zone C. Scale bar: 5 cm. (**G**) Lateral accretion surfaces in cross section. Black arrow indicates the migration of the lateral accretion. Rock pick: 33 cm.

Fig. 4. Interpretative scheme of the palaeotopography of the studied surface in which four different zones can be recognized, white arrow indicates flood flow direction. Drawings are not to scale, although the depression is approximately 0.5 m in depth.

Fig. 5. Track-bearing surface: (**A**) False-colour depth image. (**B**) Interpretative scheme showing numbered tracks; white arrow indicates flood flow direction; black arrows indicate slipping track directions; and both grey areas indicate areas without significant track impressions. (A–B) scale bar: 30 cm.

Fig. 6. (**A**) Detail of tracks 1, 2, 3, 16, 18 and 19 (**B**) False-colour depth image. of tracks 1, 2, 3, 16, 18 and 19. (A–B) scale bar: 20 cm (**C**) Detail of wrinkle marks inside track 1 from square (i) in (A). (**D**) Detail of wrinkle marks inside track 19 from square (ii) in (A). (C–D) scale bar: 5 cm. (**E**) Panoramic photograph of the slipping tracks (Zone C) closest to the surface with ripples (Zone B), white arrow indicates flood flow direction and the square

shows the location from tracks in (A). (**F**) Perspective photograph of the same slipping tracks (Zone C), marked with chalk.

Fig. 7. (**A**) Panoramic photograph of the track-bearing surface from Zone C. (**B**) Photogrammetric model of track 9 showed insquare (i) of Fig. 7A, arrow indicates a lateral acuminate impression. (**C**) False-colour depth image of track 9. (A–B) scale bar: 5 cm (**D**) Detail of tracks 4, 5, 7 and 18 showed in square (ii) of Fig. 7A. (**E**) False-colour depth image from tracks 4, 5, 7 and 18. (B–C) scale bar: 20 cm. (**F**) Detail of wrinkle marks inside track 18 (showed in square iii from D). Scale bar: 5 cm (**G**) Detail of wrinkle marks inside the track 5 (showed into the square iv from D), arrow indicates an internal rim corrugation. Scale bar: 3 cm. (**H**) Detail of wrinkle marks inside track 9, arrow indicates the inner side of the rim. Scale bar: 1 cm.

Fig. 8. (**A**) Photograph of the track-bearing level (Zone D), arrows indicate eroded ripples, where only the troughs are preserved. Scale bar: 10 cm. (**B**) Detail of a fossil wood fragment indicated in the square (i). Scale bar: 2 cm. (**C**) Detail of tracks 21 and 22 and wrinkle marks indicated in square (ii) of Fig. 8A. Scale bar: 5 cm. (**D**) Photograph in perspective of a crescent-shaped track 21. Arrows indicate boundary between track 21 and the wrinkle marks. (**E**) Interpretative scheme of track 21. (**F**) False-colour depth image of track 21. (D–F) scale bar: 5 cm.

Fig. 9. SEM photographs of both wrinkle marks (**A**–**C**) and rims (**D**) from Zone C: (**A**) Detail of a filament sheath, 15,000×; (**B**) Filament-like forms (marked with arrow) mostly parallel to the bedding plane, 15,000×; (**C**) Clusters of coccoidal forms (marked with arrow), 20,000×; (**D**) Deformed biofilm, 4000×.

Table Caption

Table 1. *Measurements and parameters of the tracks from Zone C and Zone D*

Numbers in bold indicate the elongated tracks with a length/width ratio greater than 2.

Track	Length (cm)	Width (cm)	Length/ Width	Area imprint (cm^2)	Perimeter (cm)
1	35.1	16.2	2.17	566	106
2	39.2	13.4	2.93	501	104
3	42.3	18.4	2.30	709	117
4	29.1	11.7	2.49	315	80
5	37.4 (50.5)	13.9	2.69	447	98
6	27.8	11.8	2.35	378	88
7	12.2	26.1	0.47	244	64
8	35.5	16.3	2.18	415	97
9	28.1	20.7	1.36	424	83
10	25.7	18.1	1.42	433	78
11	20.5	18.2	1.13	27	82
12	5.0	10.2	0.49	38	25
13	16.4	12.0	1.37	196	55
14	12.7	12.5	1.02	142	45
15	36.2	12.7	2.85	436	95
16	31.3	14.9	2.10	467	90
17	15.2	12.5	1.22	180	50
18	31.8	18.6	1.71	478	86
19	21.6	21.3	1.01	322	67
20	22.9	12.8	1.79	259	65
21	6.5	11.1	0.59	58	31
22	5.0	12.3	0.36	47	32
23	7.0	14.0	0.50	63	37

Table 1

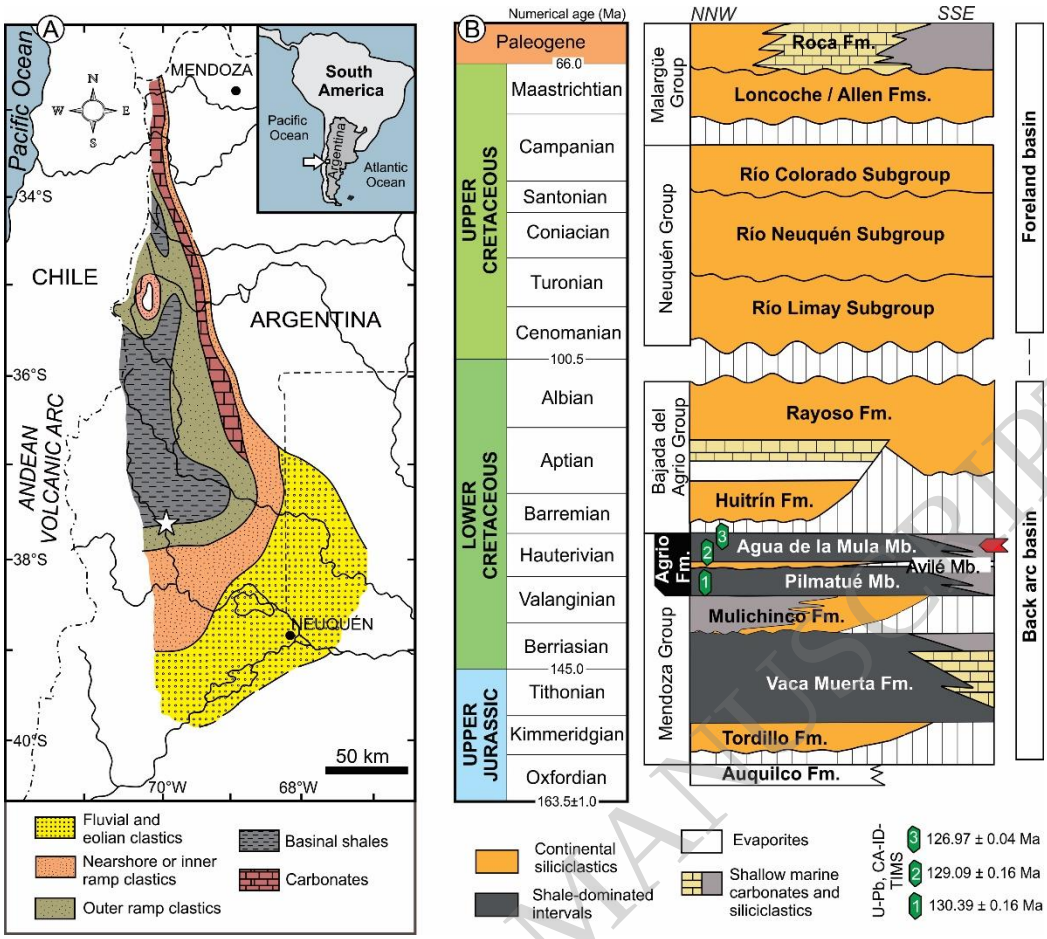

Figure 1

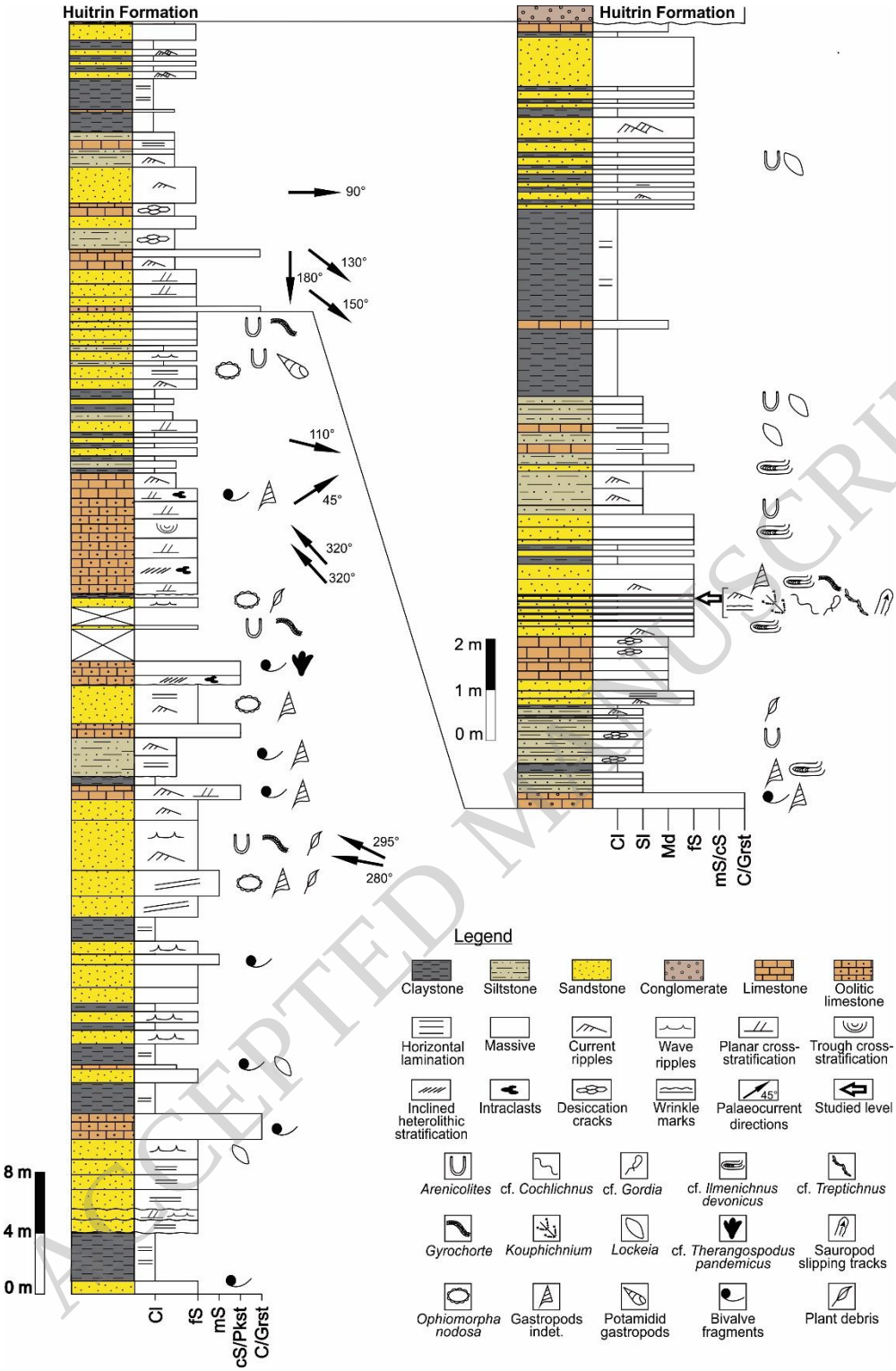

Figure 2

Figure 3

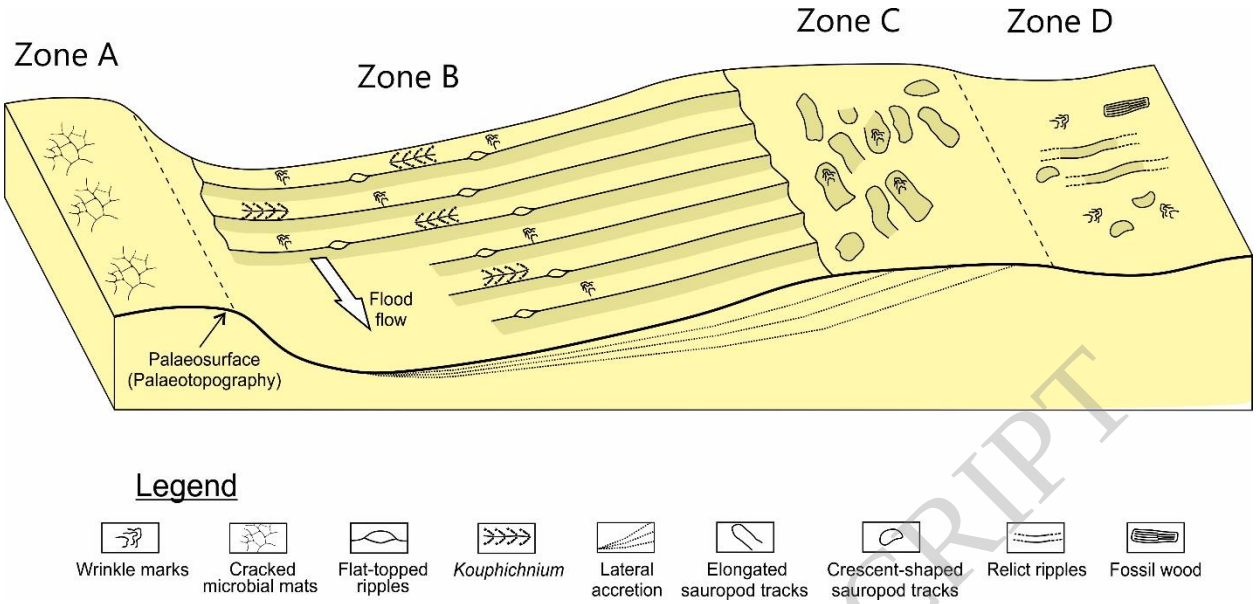

Figure 4

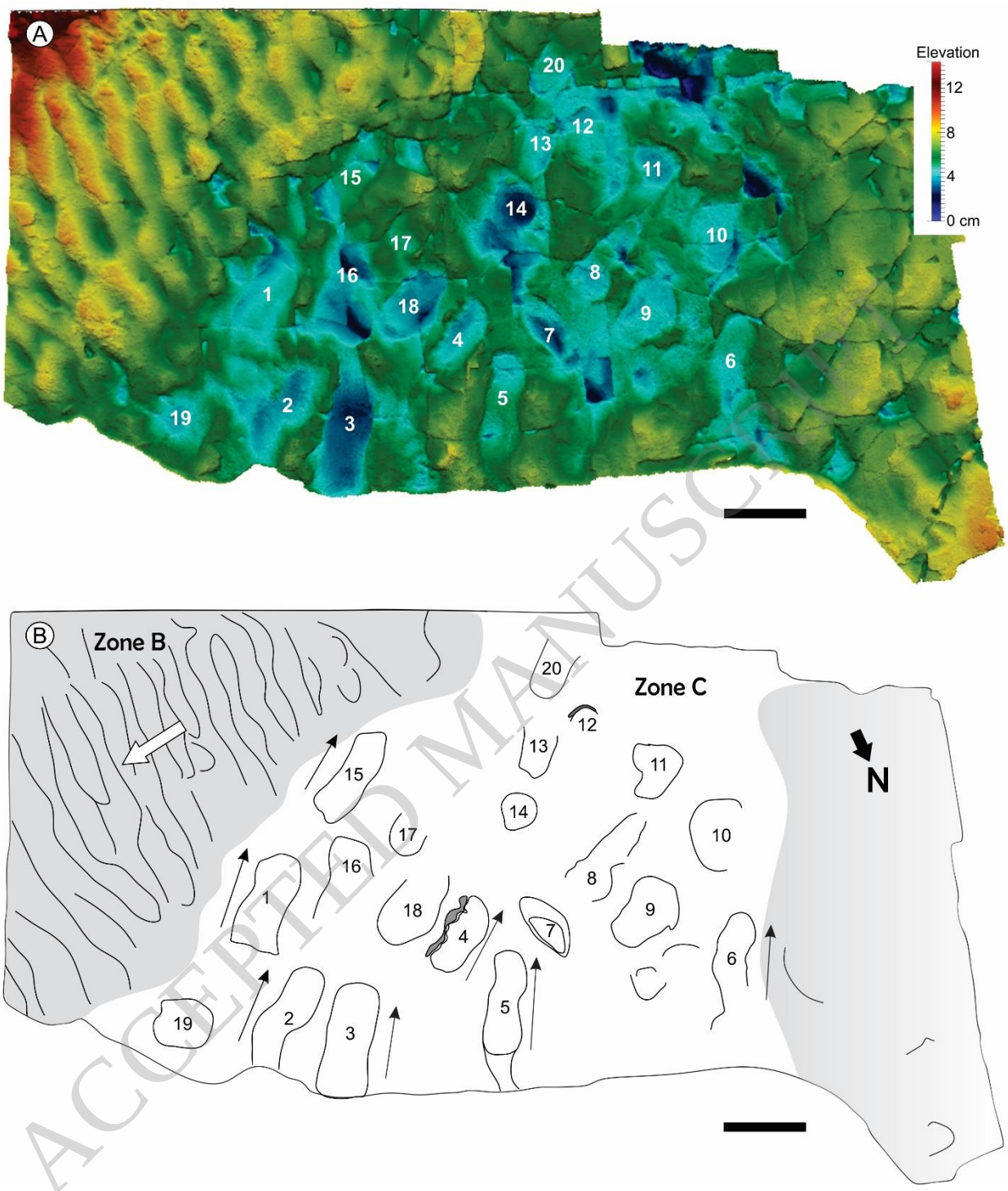

Figure 5

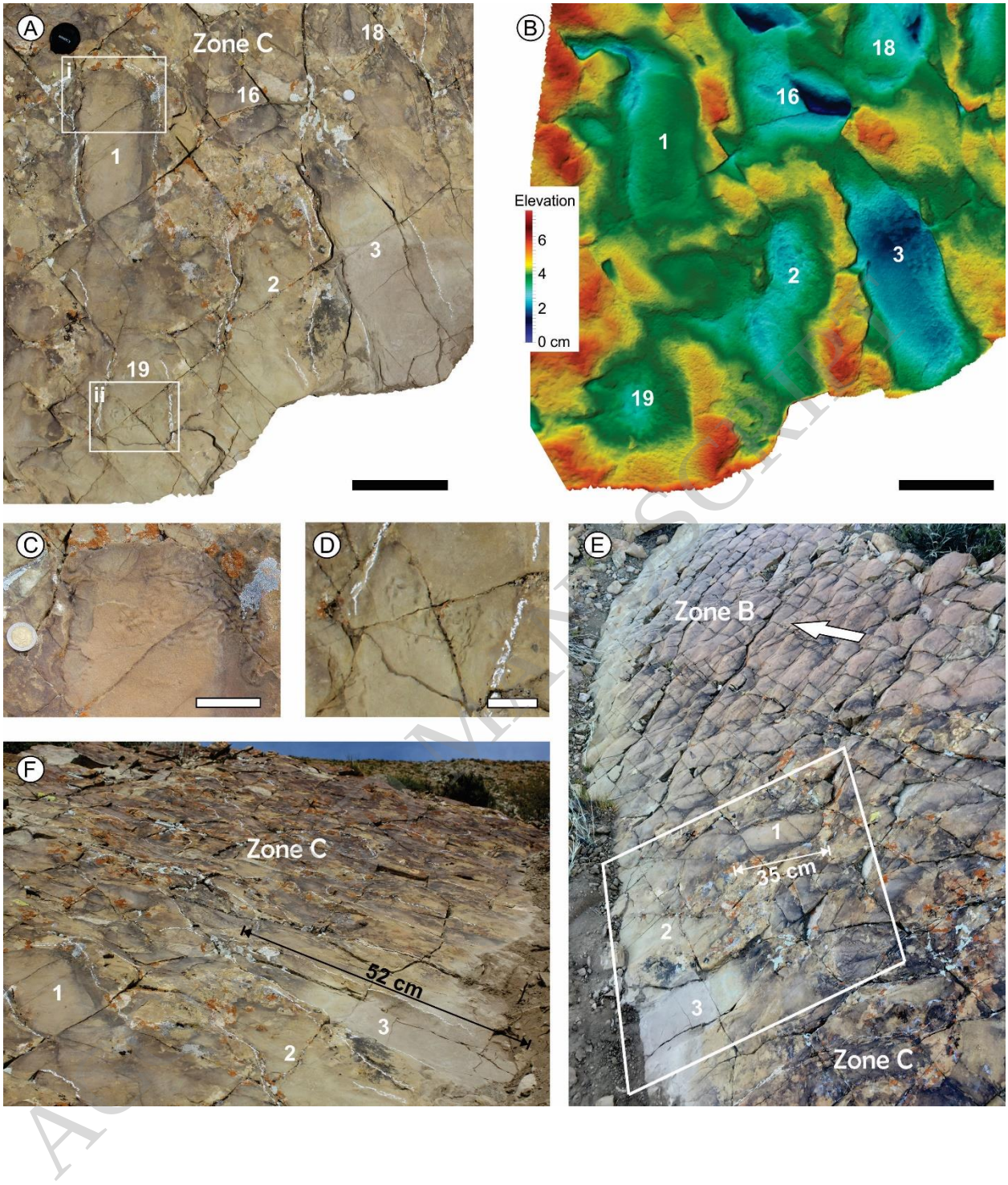

Figure 6

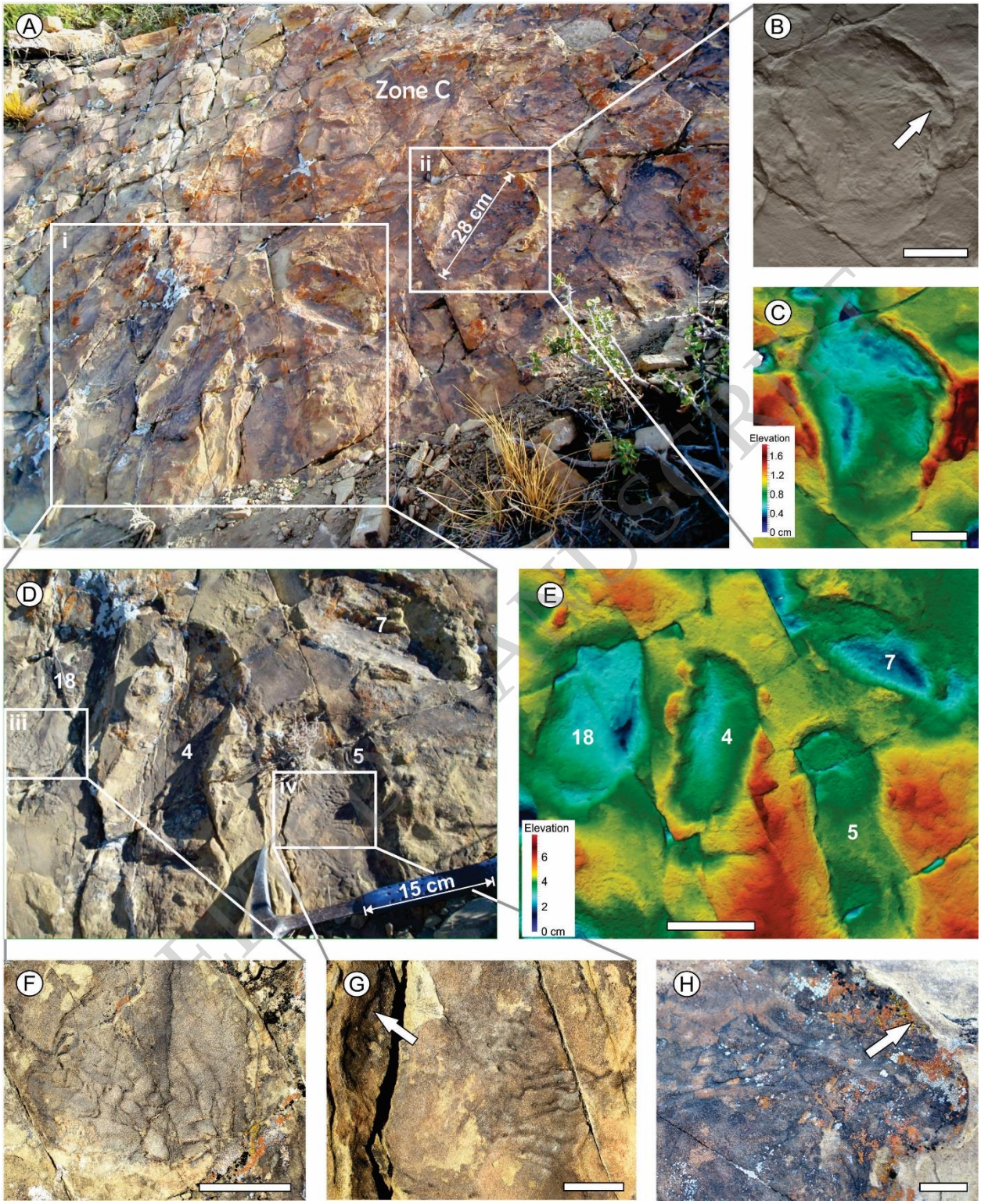

Figure 7

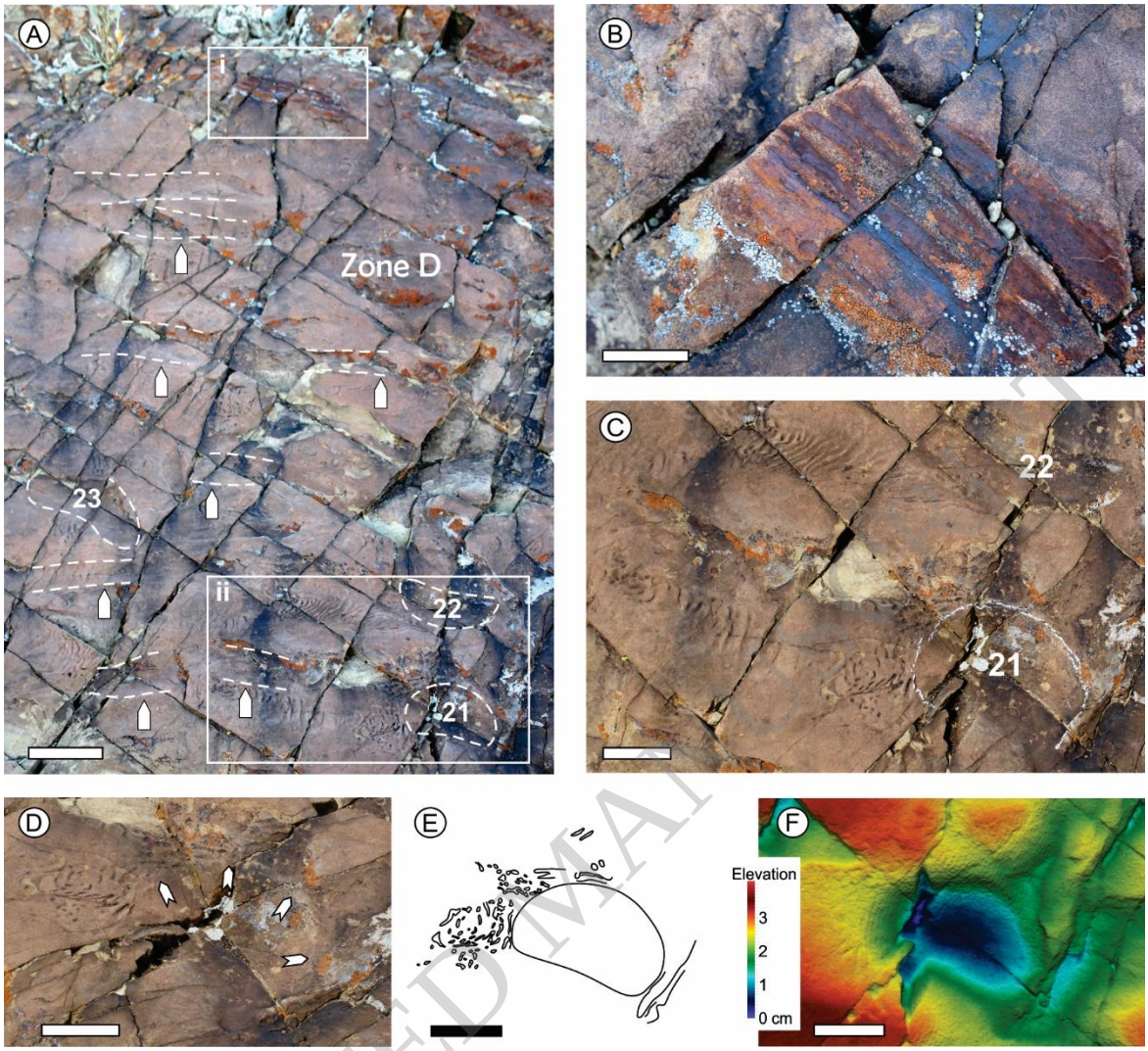

Figure 8

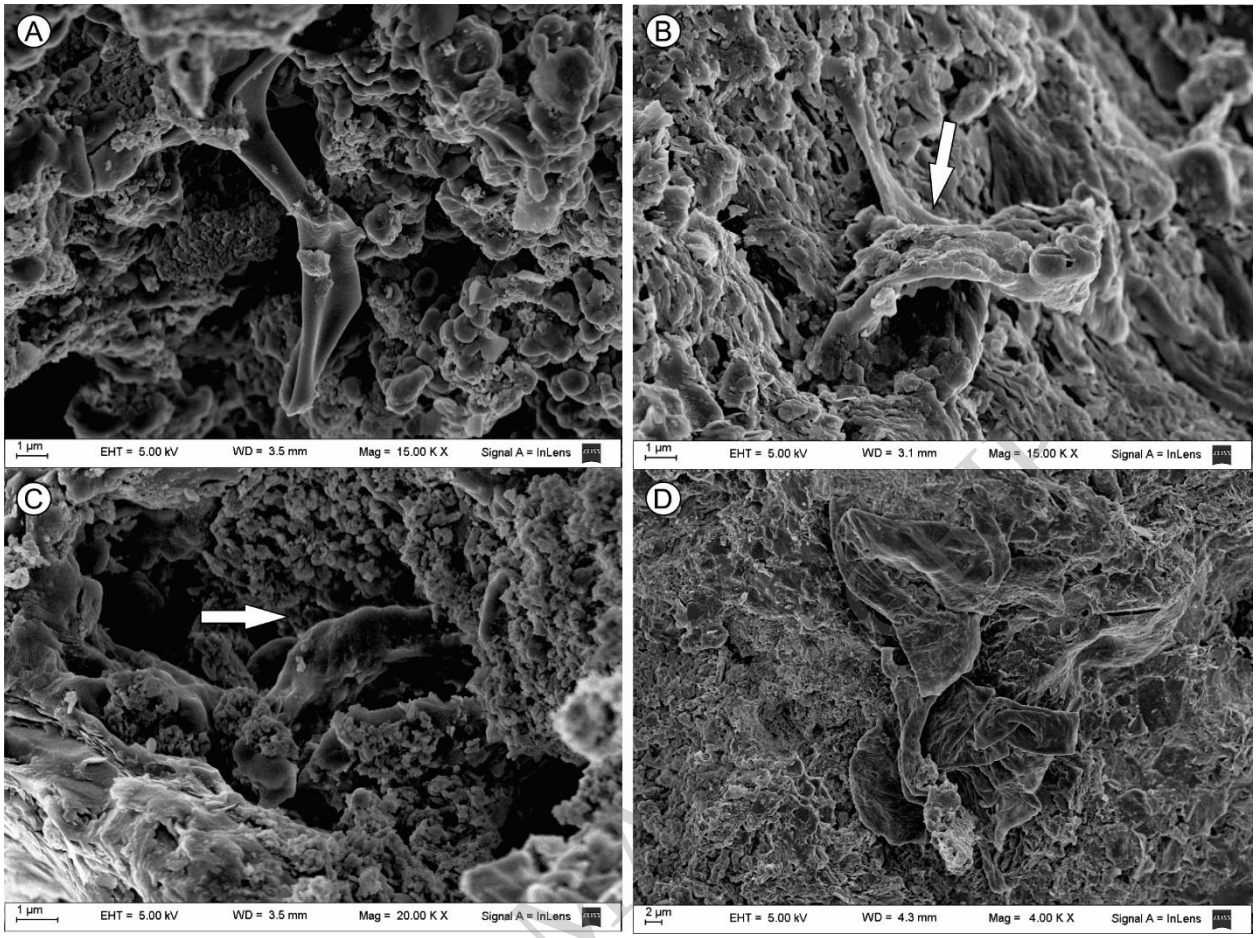

Figure 9